VIBRATION AND STRESS ANALYSIS OF MULTISTORY STEEL STRUCTURE

A Thesis By

TAMZEED AHMED ALVY

DEPARTMENT OF MECHANICAL AND PRODUCTION ENGINEERING

ISLAMIC UNIVERSITY OF TECHNOLOGY

May 2022

VIBRATION AND STRESS ANALYSIS OF MULTISTORY STEEL STRUCTURE

TAMZEED AHMED ALVY

ID: 170011063

Session: 2018-2021

Submitted in Partial Fulfillment of the Requirements for the Degree of

Bachelor of Science in Mechanical Engineering

Academic Year 2020-21

DEPARTMENT OF MECHANICAL AND PRODUCTION ENGINEERING

ISLAMIC UNIVERSITY OF TECHNOLOGY (IUT)

GAZIPUR, BANGLADESH

May 2022

CERTIFICATE OF RESEARCH

This thesis titled "VIBRATION AND STRESS ANALYSIS OF MULTI-STORY STEEL STRUCTURE" submitted by TAMZEED AHMED ALVY (170011063) has been accepted as satisfactory in partial fulfillment of the requirement for the Degree of Bachelor of Science in Mechanical Engineering.

Supervisor

____

Dr. Md. Zahid Hossain

Professor

Department of Mechanical and Production Engineering (MPE)

Head of the Department

____

Dr. Md. Anayet Ullah Patwari

Professor

Department of Mechanical and Production Engineering (MPE)

Islamic University of Technology (IUT)

DECLARATION

I hereby declare that this thesis entitled "Vibration Analysis of Multi-story Steel Structure" is an authentic report of our study carried out as requirement for the award of degree B.Sc. (Mechanical Engineering) at Islamic University of Technology, Gazipur, Dhaka, under the supervision of Dr. Md. Zahid Hossain, Professor, MPE, IUT in the year 2022

The matter embodied in this thesis has not been submitted in part or full to any other institute for award of any degree.

____

Tamzeed Ahmed Alvy

170011063

Acknowledgments

I express my gratefulness and praise to Almighty Allah for blessing me with divine guidance and love. This laid the foundation for the thesis to become a reality.

I'm truly indebted and grateful for the love that my family has provided for me throughout everything.

I am grateful and feel profound indebtedness towards my supervisor, Dr. Md. Zahid Hossain, Professor, Department of Mechanical and Production Engineering, IUT. His endless patience, scholarly guidance, constant support, extreme patience, and energetic encouragement towards the path of fruitful research has guided me in achieving this endeavor.

A special thanks to Mr. Chowdhury Said Alam, Lecturer, Department of Mechanical and Production Engineering, IUT, for helping me with the project.

I would like to extend my gratefulness and gratitude towards the senior operators and teachers at IUT workshop for helping me in constructing the experimental model and assisting me in performing the experiment. Thank you to those who have helped me along the way.

I seek profound forgiveness for any errors and mistakes in this report despite my best efforts.

Abstract

Modal parameters of structures and machines is crucial to determine the dynamic behavior during operation stages. A necessary step is to determine the dynamic characteristics and optimize the structure at its design phase to prevent any catastrophic failure. So, the purpose of this study is to focus on the modal parameters of steel structures both numerically and with experimentation and to shed some light on the equivalent stresses developed in the structure through numerical methods. Not only the modal parameters have been determined, but also the validation of the results through experiment. This will allow for accurate analysis on high-rise steel structures numerically without doing costly experiments. The mode shapes and natural frequencies of the 4-story structure for both loaded and unloaded conditions have been found through simulation in ANSYS. The first 6 modes have been extracted as these have been seen to affect the structure the most during dynamic loading condition such as earthquakes. These modal parameters have been validated using experimental method using a model 2-story structure through harmonic analysis. And finally, Von Mises stress analysis has been performed to find the relative stresses developed in the 4-story unloaded structure during different mode shapes and natural frequencies. From the research, the simulation results have been validated using the experimental data. And from the different loading condition of the structure, the different mode shapes and natural frequencies have been found. As the loading is changing from floor to floor, so is the change in mode shapes and natural frequencies. The shapes and natural frequencies greatly vary from the unloaded structure. The novelty of the research is that the modal parameters due to different loading conditions and compared those with an unloaded structure.

Table of Contents

List of Tables

List of Figures

Nomenclature

FRA	Frequency Response Analysis
HRA	Harmonic Response Analysis
CAD File	Computer Aided Design File
TMD	Tuned Mass Damper
UDL	Uniformly Distributed Load

CHAPTER 1

Introduction

Structures are basically a combination of parts joined together using various components which creates a supporting framework. This may be the part of a ship, vehicle or in this case, a building [1]. At the design phase, it is crucial to know the dynamic behavior of a structure or machine in operating conditions. This is done to prevent any unaccounted failures. Modal analysis has been the go-to method for predicting the dynamic characteristics of a structure. Not only does it show how the resonant frequencies affect the structure but also it allows the designer to identify weaknesses and strengthen them when designing. Modes, in an essence, are inherent identifiers of a structures and is deeply connected with resonance. Modes do not depend on the external loading ($f(t) = 0$) but they do change with material properties, such as density, stiffness, and damping. Modes can be determined analytically, numerically, and experimentally. Numerical methods allow for investigating complex structures easily and rapidly and does not require the cost of what experimental methods may incur. But experimental methods are important to validate the numerical results. One cannot simply accept the computer results blindly. Now, looking into the mathematical formulation will help to see how the modal analysis is carried out. A 2-story structure analysis for understanding the concept shall be considered.

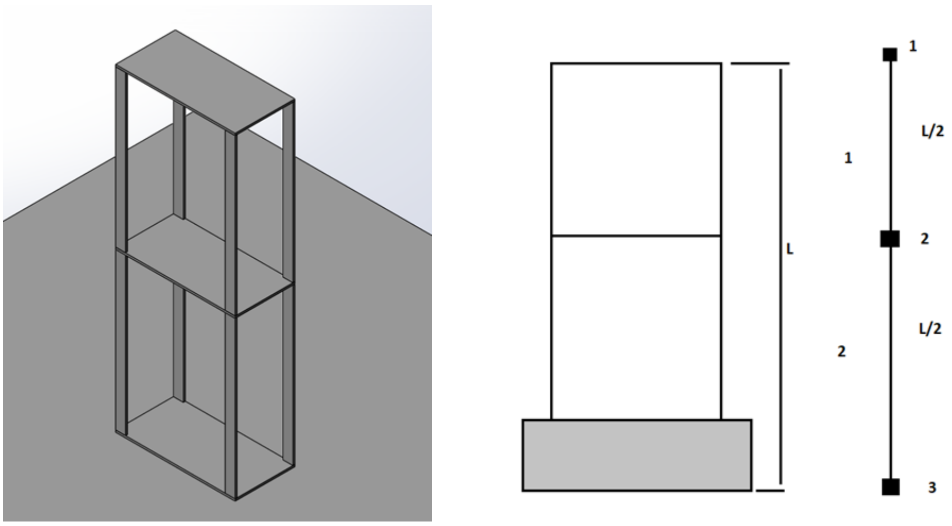

(a) (b)

Figure 1: 2-story steel structure and schematic.

Assuming stiffness to be equal on both floors, the stiffness k can be expressed as:

$$k = (2*A*E)/L \ldots (1.1)$$

Therefore, the stiffness matrices are:

$$[k^1] = [k^2] = (2*A*E)/L * \{(1, -1) ;(-1,1)\} \ldots (1.2)$$

Let, mass on each floor be:

$$m = (\rho*A*L)/2 \ldots (1.3)$$

Assuming the masses to be equally distributed, the mass matrices are:

$$[m^1] = [m^2] = (\rho*A*L)/12 * \{(2, 1) ;(1, 2)\} \ldots (1.4)$$

Through direct assembly procedure, matrices can be written globally. For the stiffness matrix:

$$[K] = (2*A*E)/L * \{(1, -1, 0) ;(-1, 2, -1) ;(0, -1, 1)\} \ldots (1.5)$$

Similarly, for the mass matrix:

$$[M] = (\rho*A*L)/12 * \{(2, 1, 0) ;(1, 4, 1) ;(0, 1, 2)\} \ldots (1.6)$$

By definition:

$$[M]. [\ddot{U}] + [K]. [U] = 0 \ldots (1.7)$$

Replacing equation (1.6) into (1.7) yields:

$$(\rho*A*L)/12 * \{(2, 1, 0) ;(1, 4, 1) ;(0, 1, 2)\} * \{(\ddot{U}_1) ;(\ddot{U}_2) ;(\ddot{U}_3)\} + (2*A*E)/L * \{(1, -1, 0) ;(-1, 2, -1) ;(0, -1, 1)\} * \{(U_1) ;(U_2) ;(U_3)\} = \{(0) ;(0) ;(0)\} \ldots (1.8)$$

Equation (1.1.8) represents a second-order, linear, ordinary differential equation. Since the fixed end displacement is 0, $U_1 = 0$. The equation (1.8) can be rewritten as:

$$(\rho*A*L)/12 * \{(4, 1) ;(1, 2)\} * \{(\ddot{U}_2) ;(\ddot{U}_3)\} + (2*A*E)/L * \{(2, -1) ;(-1, 1)\} * \{(U_2) ;(U_3)\} = \{(0) ;(0)\} \ldots (1.9)$$

Sinusoidal response due to free vibration can be expressed as:

$$U_2 = A_2 * \sin(\omega t + \phi),\ U_2 = A_3 * \sin(\omega t + \phi) \ldots (1.10)$$

Differentiating equation (1.10) and substituting it into (1.9) yields:

$$-\omega^2 * \{(4, 1) ;(1, 2)\} * \{(A_2) ;(A_3)\} * \sin(\omega t + \phi) + (24*E/\rho*L^2) * \{(2, -1) ;(-1, 1)\} * \{(A_2) ;(A_3)\} * \sin(\omega t + \phi) = \{(0) ;(0)\} \ldots (1.11)$$

A_2 and A_3 are the vibration amplitudes of the nodes and $-\omega^2$ is the harmonic circular frequency. The phase angle is described by ϕ. This equation has no trivial solutions. If $\lambda = 24*E/\rho*L^2$,

$$7*\omega^4 - 10*\lambda*\omega^2 + \lambda^2 = 0 \ldots (1.12)$$

The roots of the equation are:

$$\omega^2{}_1 = 0.1082*\lambda \text{ and } \omega^2{}_2 = 1.3204*\lambda \ldots (1.13)$$

The natural circular frequencies from equation (1.1.13) can be found as:

$$\omega_1 = (1.611/L) * \sqrt{E/\rho} \text{ and } \omega_2 = (5.629/L) * \sqrt{E/\rho} \text{ rad/sec} \ldots (1.14)$$

This is the formulation of the theoretical modal analysis. ω_1 and ω_2 are the eigenvalues of the structure and the amplitude ratio A_2/A_1 represents the eigenvector or mode shapes [2].

Structural Vibration and Control: Two factors control the amplitude and frequency of structural vibration. These two factors are the excitation applied and the response to that excitation. Changing either of these will affect the vibration stimulated. In many forms these excitations may appear such as ground foundation vibration, cross winds, waves and currents, earthquakes, and sources withing the structures such as moving loads and machineries. The nature of these vibrations may be periodic, harmonic, impulsive or random. The response of the structure depends on the application and location of these exciting forces. The dynamics depend on the natural frequency and the damping [1].

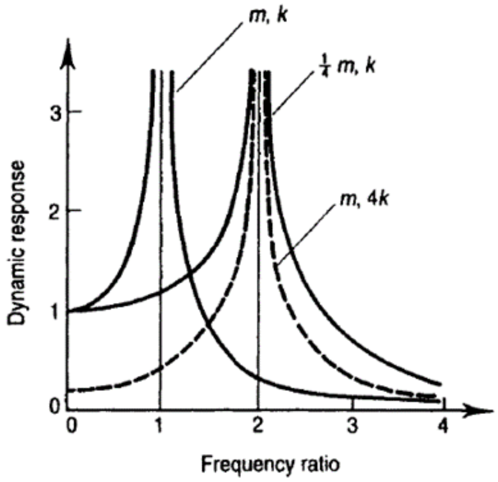

Figure 2: Effect of mass and stiffness on dynamic response of structure[1]

Early structures, being built from heavy timbers, casting, and stonework, made them heavy and highly damped. Except for wind, gravity and seismic loads, the vibration sources were very few during the times before the industrial revolution. This made them structurally less responding to dynamic loading. Building now are made with more knowledge than ever before. Lightweight materials and better design make buildings different than before. Since then, excitation has been increased while the structural mass decreased and damping increased. Many structures are being built without extensive vibration analysis since the necessary dynamic performance is acceptable. Still, structures have failed or have not met their design criteria due to resonance, fatigue, or excessive vibration. Therefore, it is necessary to perform vibration analysis of structures at their design phase [1]. The design of steel buildings become a broad topic when considering the seismic effects. With keeping that in mind, the designs have been focusing on seismic-force resistant systems. Some of these notable systems described by Chia-Ming Uang et al. include moment frame systems, concentrically braced frames, eccentrically braced frames, buckling restrained braced frames and shear wall systems [3].

Theodore V. Galambos describes the recent research and design of steel buildings in the USA. In his studies, he has described the researches that is being conducted on the steel frames and members, cold-rolled steel structures, steel-concrete composite structures, connections and the impact of seismic forces, research on high performance steel and so on. [4]

To reduce unwanted situations and creating long lasting structures, it is necessary to devise ways to control or reduce these phenomena. One way may be to designing a stage that separates the structure to reduce incoming vibration. Another way is to alter the mass, stiffness or increasing the damping the structure or removing any sources of excitation forces from the weakest parts after reviewing it [1]. To decrease the structural vibration, many methods have been in development since the 1980s. Khaled Ghaedi et al. has talked about the application of active and passive of control of steel structures. In active vibration controlling, the essential dynamic loading data is received by the controller and through actuators, the forces are countered. Various mass dampers, such as active mass damper, active tuned mass damper, active tendon damper etc. have been in use to improve the serviceability and longevity of the structure. Passive vibration control systems are embedded into the structural members. Usually TMD or tuned mass dampers are used with optimum damping ratio, TMD mass etc. [5] The use of smart materials have been seen in controlling the building vibrations. G Song et al. have presented the use of piezoceramic smart materials for active vibration control. These are low-cost, light-weight, easy to incorporate and can be available in different configurations such as patch, stack, micro-fiber composite etc. [6] . The energy dissipation capacity of a building is very important during earthquakes. To design the energy dissipation rate, a 3-stage grip is introduced within each story to control the vibration. These have been proven as satisfactory under high dynamic loading [7]. There has been development in tuned mass dampers. The passive mass dampers include TMD, TLCD, TLCBD, PTLCD etc. For active mass dampers, ATMD, MRD, MR-TMD, NSD, VD-STMD etc. are being used [8].

Modal and Frequency Response Analysis: Among many reasons, rotary, and static equipment or in our case, multi-story steel structures, fail when they are subjected to high vibration during operation that causes them to vibrate at near-resonance or resonance frequency. One can reduce these high levels of perturbation forces by balancing, aligning, or adding flow straighteners for rotary machines. Sometimes altering the frequency of the perturbation forces become impossible. That's when natural frequency of the structure is altered to stabilize it. But this is not possible to do without knowing the mode shapes where mode shapes or deflection allows one to determine the maximum deflection of the structure. By knowing that, one can either stiffen that location or make it flexible. So, the exploration of the natural frequencies and mode shapes can be called in short as 'modal analysis.' Modal analysis may be performed analytically or through finite element analysis. For simple structures, it is easy to perform analytical calculations. But structures with complex geometry, multi-degrees of freedom make analytical process impossible. That where FEA comes into play. With its versatility, one can easily determine the modal parameters. But this too has its limitations when the boundary condition selection becomes a challenge, and the calculation becomes very large. That's when experimental methods come into the picture. To validate the numerical results, it is essential to perform experiments. The experimental procedure can be of two types. In one method, a harmonic excitor is used for applying a constant load to measure the modes. Another method is using an impact hammer and analyzing the signal in FFT to determine the modes. Both methods have their pros and cons and depending on the use cases, either of the two methods can be used quite effectively.

A system will respond according to various input frequencies. At some frequencies the vibration may be seen to amplify considerably and may attenuate to the vibration. The way the output of the system responds to the input is termed as the frequency response of the system. FRF is the relationship between input and output in the Fourier domain. This relation can be written as:

$$Y(j\omega) = H(j\omega) * X(j\omega) \quad \dots (1.15)$$

$X(j\omega)$ is the input or excitation force, $Y(j\omega)$ is the system output or vibration, and $H(j\omega)$ is the FRF.

Since we have evaluated our experiment with sinusoidal excitation, let us take a glimpse into the mathematical formulation of the FRF using sinusoidal-force excitation.

Let the vector be: $F = F_o*e^{i\omega t}$ … (1.16)

The velocity vector is $\dot{x} = i*\omega*x$ and acceleration vector is $\ddot{x} = -\omega^2*x$.

Therefore, the mechanical impedances of the spring, mass and damper systems are:

Spring = k, Mass = $-m*\omega^2$, Damper = $i*c*\omega$.

Expressing the harmonic-forcing function as $F(t) = F_o*e^{i\omega t}$, we get the equation of motion to be:

$$m\ddot{x} + f\dot{x} + kx = F_o*e^{i\omega t} \ldots (1.17)$$

By assuming particular solution $x_p(t)$:

$$x_p(t) = X*e^{i\omega t} \ldots (1.18)$$

Substituting equation (1.18) into equation (1.17) yields:

$$X = F_o/((k-m*\omega^2) + if*\omega) \ldots (1.19)$$

Through mathematical manipulation of equation (1.19),

$$X = F_0* [k-m*\omega^2/ (k-m*\omega^2)^2 + f^2*\omega^2 - i* f*\omega/ (k-m*\omega^2)^2 + f^2*\omega^2] \ldots (1.20)$$

The steady-state solution is:

$$x_p(t) = (F_o/\sqrt{[(k-m*\omega^2)^2 + (f*\omega)^2]}) *e^{i(\omega t-\phi)} \ldots (1.21)$$

These manipulations are done to bring out the frequency response function.

The steps for finding it are left for the reader as an exercise. The final equation that can be found for FRF is: $x_p(t) = (F_o/K) *| H(j\omega) | *e^{i(\omega t-\phi)} \ldots (1.22)$

The use of this function, $H(j\omega)$, is made in the experimental determination of system parameters such as m, f and k since it contains the magnitude and phase information of the steady-state response [9].

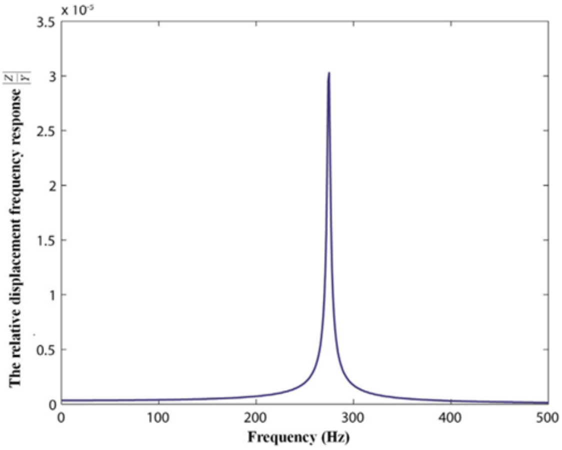

Figure 3: The frequency response function of a linear mechanical single degree of freedom spring-mass-dashpot system shown through MATLAB programming for understanding purposes[10]

Mathematical Models: Now, the discussion continues for the mathematical models that have been incorporated into finding the mode shapes, natural frequencies, harmonic response, and stresses.

Block-Lanczos Mode Extraction Method: An adaptation of the power method, the Lanczos algorithm is an iterative method used to find the m 'most useful' eigenvalues and eigenvectors of an n*n Hermitian matrix and m is most of the time smaller than n. A natural extension to the original Lanczos algorithm can be found using the Block-Lanczos algorithm for multiple vectors. K and M, a given pair of matrices, and a set of k starting vectors R = [r1, r2, … rk], the method generates n*k matrix sequence, [R, K-1MR, (K-1M)2. R, … (K-1M)j.R], during j iterations. This is known as the Kyrlov sequence and the set of vectors in the sequence is simply a block. This method is a two-step procedure. First, a set of vectors in individual blocks are orthogonalized and then it is imposed among the blocks. After that, a linear combination is taken, and a new set of blocks are obtained which are orthogonal. The derivation of the Block-Lanczos method is given in the appendix. In summary, to derive the Gj+1 vector using the Lanczos algorithm, the following sequence of equations may be used [11].

$$\bar{R}j = K-1MGj \ldots \ldots \ldots (1.23)$$

$$Rj = \bar{R}j - GjAj - Gj-1\ Bj \ldots \ldots \ldots (1.24)$$

$$\text{Where, } Rj-1 = GTjM\bar{R}j \ldots \ldots \ldots (1.25)$$

$$\text{Factor } Rj-1 = GTjBj \ldots \ldots \ldots (1.26)$$

$$Rj = Gj+1\ Bj+1 \ldots \ldots \ldots (1.27)$$

Mode Superposition Method: There are two methods to perform harmonic response analysis. One is using the mode superposition method and the other is full harmonic. The full harmonic is costly is terms of computer memory and processing time. Therefore, mode superposition method is used for its advantages in terms of cost and efficiency. To measure the dynamic response efficiently, the mode superposition method has been used. It can allow for approximating the dynamic response of a structure using a small number of the eigenmodes. When the frequency content of the loading is limited, the mode superposition method becomes very useful. Its usefulness can be seen when performing analyses in the frequency domain since the loading frequencies are already known.

Von Mises Stress Analysis: Different behavior when non-simple tension or non-uniaxial stress applied to ductile material are much larger than the ones observed in the simple tension experiment and that gave birth to the maximum distortion energy theory. Widely used for metals and other ductile materials, the criterion for yielding is the von Mises stress. This criterion states that the stress components acting on a body being greater than the criterion will cause yielding of the body. This is given by:

$$1/6[(\tau_{11} - \tau_{22})^2 + (\tau_{22} - \tau_{33})^2 + (\tau_{33} - \tau_{11})^2 + 6*(\tau^2_{12} + \tau^2_{23} + \tau^2_{13})] = k^2 \ \ldots \ (1.28)$$

τ is the stress tensor and k are found through experiment. k is defined from uniaxial stress where expression (1.28) reduces to:

$$\tau^2_y/3 = k^2 \ \ldots \ (1.29)$$

if simple tension elastic limit is reached, the above expression becomes:

$$S^2_y/3 = k^2 \ \ldots \ (1.30)$$

Substituting expression (1.30) into (1.28) yields:

$$1/6[(\tau_{11} - \tau_{22})^2 + (\tau_{22} - \tau_{33})^2 + (\tau_{33} - \tau_{11})^2 + 6*(\tau^2_{12} + \tau^2_{23} + \tau^2_{13})] = S^2_y/3 \ \ldots \ (1.31)$$

Or finally:

$$\sqrt{}\ (\tau_{11} - \tau_{22})^2 + (\tau_{22} - \tau_{33})^2 + (\tau_{33} - \tau_{11})^2 + 6*(\tau^2_{12} + \tau^2_{23} + \tau^2_{13})/2 = S_y \ \ldots \ (1.32)$$

The von Mises stress is defined as:

$$\tau^2_v = 3k^2 \ \ldots \ (1.33)$$

Therefore, the von Mises yield criterion is also rewritten as:

$$\tau_v >= S_y \ \ldots \ (1.34)$$

So, if the von Mises stress is larger than the simple tension yield limit, it is expected that the material will yield [12].

CHAPTER 2

2.1 Research Background

It is important to evaluate the modal parameters of the structure in its design phase. When designing frames, considering the rigid or pinned joints, S. Chan [13] has shown that the assumption may not be justifiable for certain reasons. His studies have shown by using matrix method of analysis, the dynamic characteristics of steel frames can be assessed which is crucial for determining the vibration properties. The soil-foundation-structure-interaction is an important part of the dynamic properties of the structure under seismic loading. B. Vivek et al. [14] has shown that the fundamental natural frequency increases up to 20% when the base is fixed compared to when it is resting on a soil base. Similar effects have been seen when the structure is resting on loose sand compared to rigid sand base. The mode shapes are also affected by the various loading conditions. Loading can be in the form of wind induced loads, gravity loads, seismic load etc. Yin Zhou et al. [15] used high frequency base balance data to obtain the response during wind loading from the non-ideal mode shapes and compared to the ideal mode shapes of the building. Another study done by Yin Zhou et al. [16] focuses on the torsional effects of wind loading on the building. Due to the unbalanced distribution of the instantaneous pressure on the building surface, the torsional response is caused by wind effects. In this study, a framework is provided for estimating the torsional effects by utilizing the aerodynamic loading data base to be incorporated into the building codes. Human loading also affects the mode shapes of buildings. A numerical investigation done by S. Silva et al. [17] looks at the dynamic characteristics of the floors of the building during human loading. From the study, it has been found that the loading pattern heavily affects the response, and the loading must be realistic for a comprehensive vibration evaluation. In a study by Yunsang Kwak et. al [18] found through impact loading that the different loading on the lower and higher floors of a 12-story building affected the vibration propagation levels. Various other research have been conducted on the stability and operability of buildings under wind loading [19]–[23]. Gravity loads are also a contributing factor in the dynamic characteristics of buildings. They play an important role on the linear and non-linear behavior of buildings during earthquake. A study by M. Shahin et. al [24] shows that the gravity forces are an important parameter. Gravity adds a moment distribution which is a function of relative shear in the walls. Similar studies have been done that describes the effect of gravity during seismic loading. [25], [26].

2.2 Significance of The Research

From literature review it is seen that, there are few papers directly discussing on the mode shapes and natural frequency of the steel structures. These parameters are important when considering the design of buildings. Only notable literature that has been found is by M.L Chandravanshi et al. [2] which focuses on the modal parameters that have been verified through both simulation and experiment. In that work, the effect of loading criteria has been studied as well.

This study focuses on the modal parameters of 4-story structures. It investigates the modal parameters for unloaded conditions as well as the differently loaded conditions of the structure. The change in natural frequency for unloaded structure and loaded structure has been observed. It has been seen that the natural frequency and mode shape change significantly with the change of loading conditions in the structure. From stress analysis, the von Mises stresses developed in the unloaded structure have been found through simulation.

2.3 Objectives

- To find the modal parameters, such as mode shapes and natural frequency,
- To the study the loaded and unloaded conditions,
- To determine the change in mode shapes and the natural frequency for the various loading combination of the loaded structure,
- To identify the Von Mises stresses developed in the unloaded structure to understand the stress distribution throughout the structure and
- To validate the simulation results by experiment.

2.4 Methodology

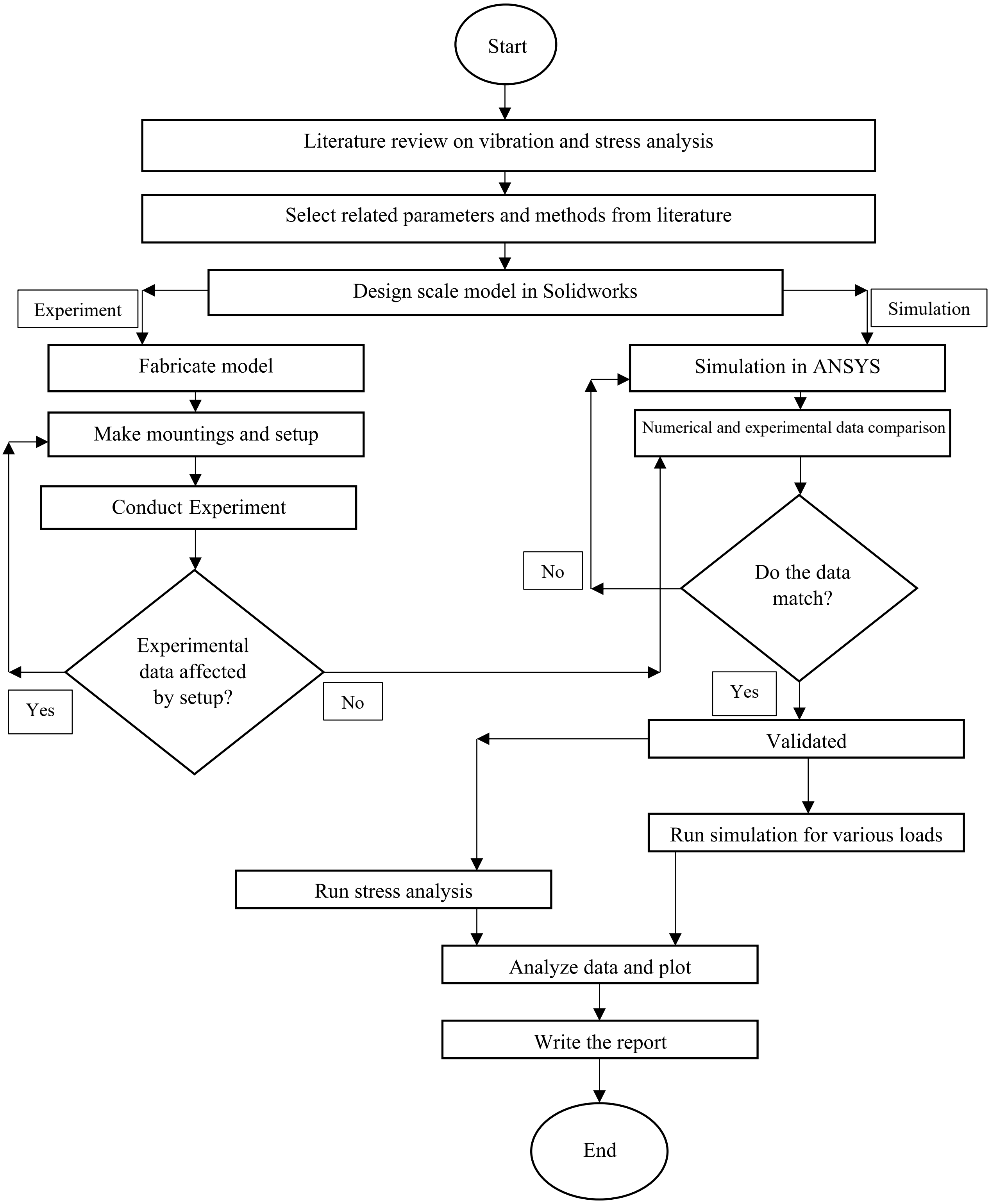

Figure 4: Flowchart of Methodology

CHAPTER 3

Geometries and Specifications

For simulation purposes, a simplified version of a steel structure has been modelled using the Solidworks 2017 design software. It's made up from floors and columns. The floors and columns are welded at their interface of connection. The bottom floor is level zero. The floors and columns have been designed to specification according to the parameters of M.L Chandravanshi et al. [2] with slight modifications. The floors are 5 mm thick with dimensions of 300×150 mm^2 and the columns are 392.5 mm high with a cross sectional area of 25×5 mm^2. Two types of structures have been considered. Those are: unloaded structure and loaded structure in various combinations. The loaded structure has a similar geometry to that of the unloaded structure but in each floor, in various combinations, it has been loaded with a uniformly distributed load of 3.53 Kg. The material for unloaded and unloaded structures have been used as mild steel. As mild steel is available and cost effective, the material has been chosen based on these conditions.

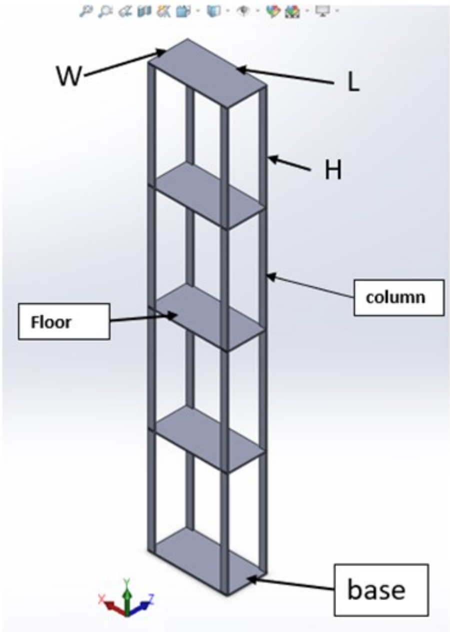

(a) Unloaded structure

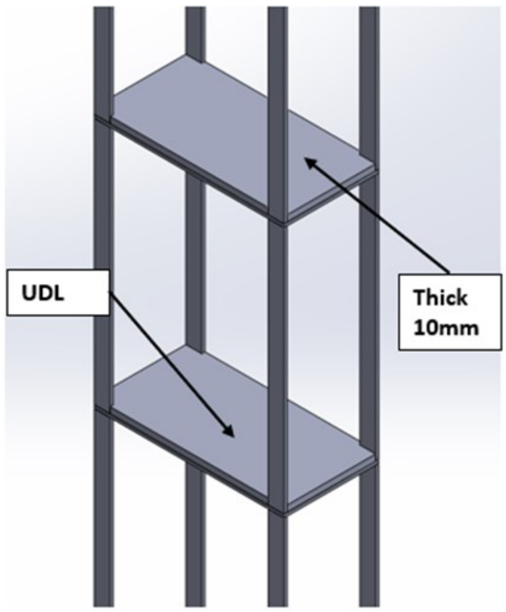

(b) Loaded Structure

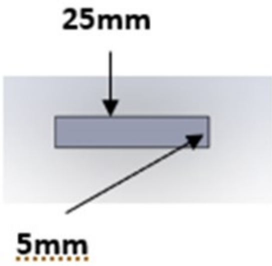

(c) Column Cross-section

Figure 5: 4-story structure modelled in Solidworks 2017.

The loaded structure has been loaded in various combination. And each combination has been studied. The UDL has been placed on the floors. The loading has been done for single floors, double floors, and triple floors. So, in some cases, the building is loaded in single floors from floor 1 to 4 and in some cases, three floors are loaded simultaneously in different combinations. The loads are made from mild steel which is the same material of the structure.

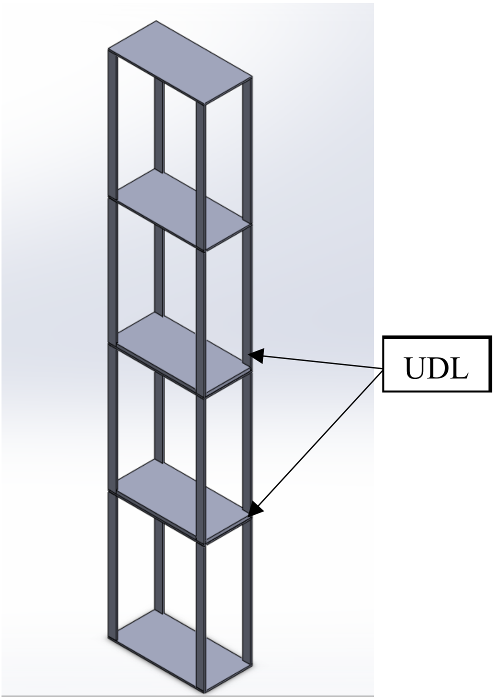

(a) Floor 1 and 2 loaded with UDL

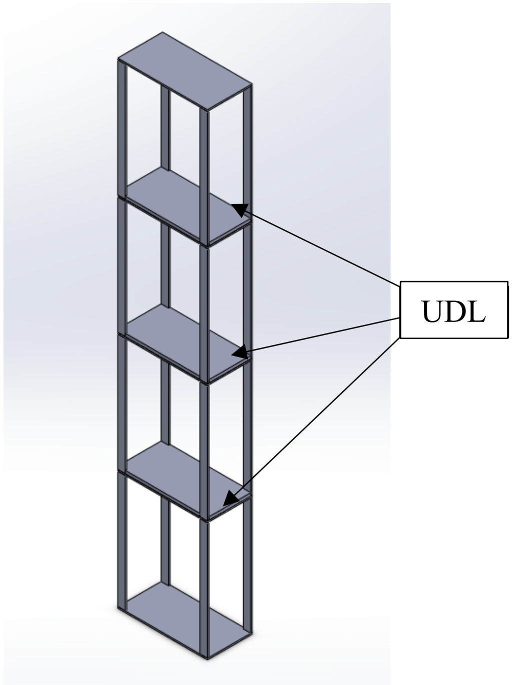

(b) Floor 1, 2 and 3 loaded with UDL

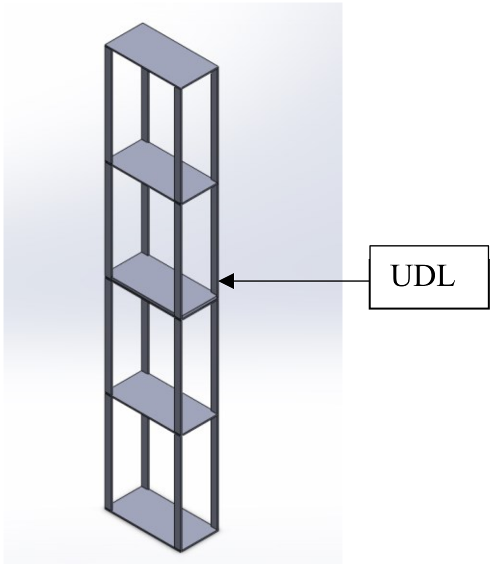

(c) Floor 2 loaded with UDL

Figure 6: Different loading conditions show for the 3 different conditions.

The geometry specification and material properties are shown in the tables below. The tables contain the floor dimensions, column dimensions and UDL dimension. The total height of the structure, both loaded and unloaded, is 1595 mm.

Table 1: 4-story structure geometry specifications for unloaded and loaded structure.

Description	Length	Width	Thickness/Height
Floor	300 mm	150 mm	5 mm
Column	25 mm	5 mm	392.5 mm
UDL Load	78.4 Kg/m^2		
Total Height of Structure	1595 mm		

Mild steel has been used as material. This material is easily available and low in cost. So, in the simulation, the standard mild steel data has been taken. Here, the important factors are density, Young's modulus and Poisson ratio. [27]

Table 2: Material properties of the 4-story unloaded and loaded structure.

Material	Mild Steel		
Property	Symbol	Value	Unit
Density	ρ	7800	$Kg.m^{-3}$
Young's Modulus	E	2.1E+11	Pa
Poisson Ratio	υ	0.295	-
Bulk Modulus	K	1.5447E+11	Pa
Shear Modulus	G	7.3359E+10	Pa
Thermal Expansion coefficient	α	1.2E-05	C^{-1}

CHAPTER 4

4.1 Simulation Setup

To calculate the mode shapes and natural frequencies numerically, ANSYS 2020 has been used for the simulation procedure. In ANSYS Workbench, the integrated ANSYS Mechanical Module for modal analysis 'MODAL' has been used. And to compute the frequency response of the structure, the 'HARMONIC RESPONSE' module has been used. The figure below shows the Workbench interface. The modal analysis is coupled to the harmonic analysis.

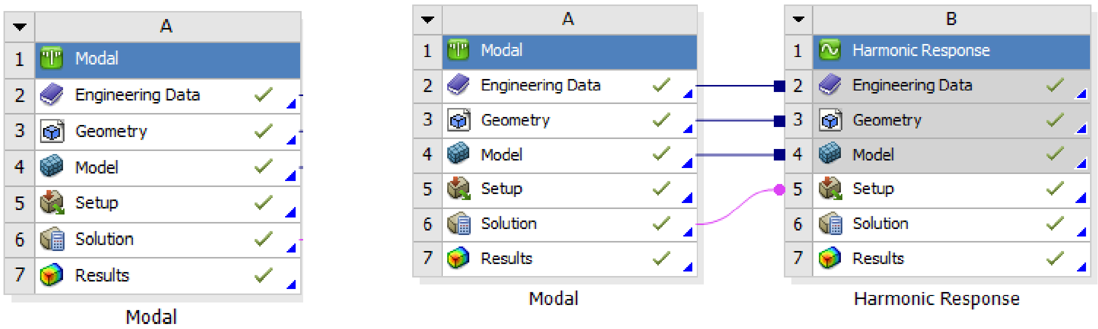

(a) Modal analysis module

(b) Harmonic response analysis coupled with modal analysis

Figure 7: ANSYS 2020 Workbench Interface

4.1.1 Engineering Data

The engineering data has been chosen as mild steel. The material data has been selected from the ANSYS library. Any other environmental effects, temperature, electro-magnetic effects etc. have been excluded from the analysis.

4.1.2 Geometry

The 3D model has been imported into ANSYS Workbench in the IGS or Initial Graphics Exchange format. It is a 2D-3D design exchange file format which is independent of source file format. It allows for exchange of design information about, in our case – wireframes, between two independent systems.

4.1.3 Meshing

The most important step is the meshing of the 3D model. A perfect mesh yields a proper solution. For this model, since the geometry is very simple, the program-controlled mesh settings have been chosen.

Table 3: Mesh generated for the 4-story structure

Settings	Description
Physics Preference	ANSYS Mechanical
Element Type	Rectangular
Element Order	Program Controlled
Element Size	5-millimeters
Number of Nodes	116518
Number of Elements	15352

Table represents the mesh parameters for the simulation. Element size has been set to 5-millimeters as it has been the best size to perform the simulation with minimum computing cost and produce reliable results.

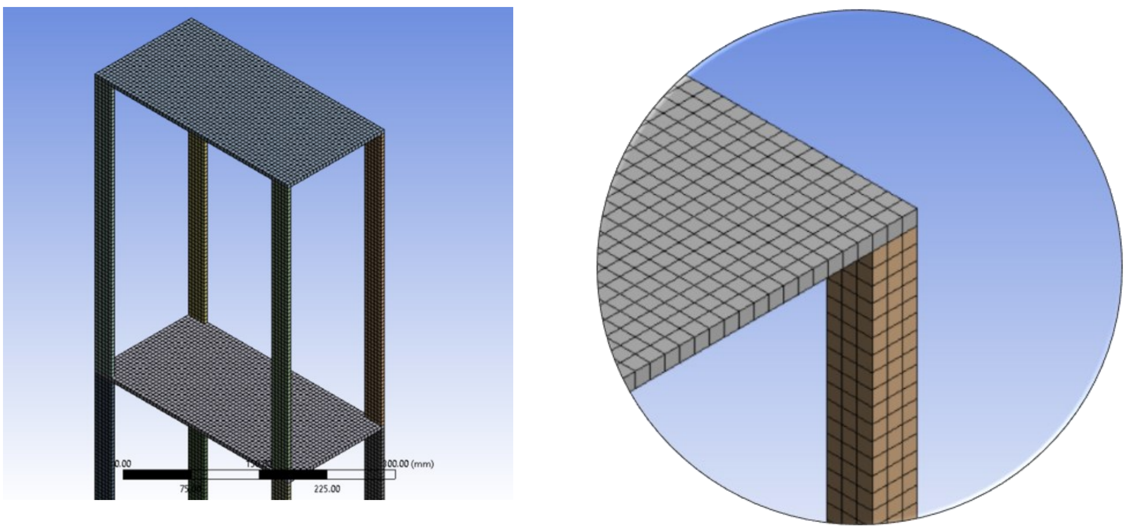

(a) Meshing of the structure (b) Close up view of mesh

Figure 8: Mesh generated for analysis purposes.

4.1.4 Boundary Conditions

For the simulation to be run, necessary boundary conditions have been applied. The base of the structure has been fixed. Rest of the structure is set free. The columns have been welded to the floors. All the other conditions have been kept as default.

4.2.1 Modal Analysis

To perform the modal analysis, the solver has been set to extract the first 6 modes. Here, the 'Block-Lanczos mode extraction method' has been used as the solver. No damping has been incorporated. It took 14 seconds to complete the mode extraction.

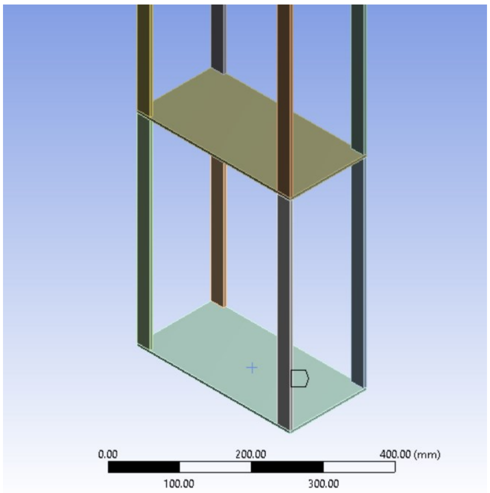

Figure 9: Fixed support applied at the base plate for analysis purpose.

4.2.2 Harmonic Analysis

For the harmonic response analysis, frequency levels from 0 Hz to 50 Hz has been chosen with linear frequency spacing. The solution intervals have been chosen to be 200. The solver type has been set to 'mode superposition method.' No damping has been incorporated. Pressure of 5 MPa has been added to the right column to provide a constant sinusoidal load on the structure column. It took 2 minutes to complete the solution.

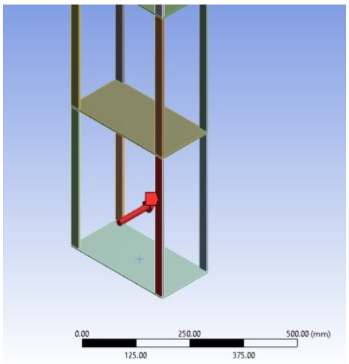

(a) Point of application

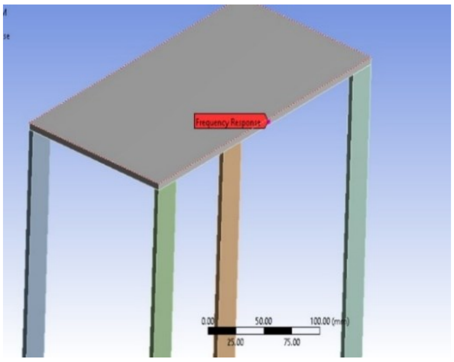

(b) Probe for data collection

Figure 10: pressure application face and data collection probe at the top floor.

4.2.3 Von Mises Stress Analysis

The equivalent von-Mises stress has been determined from the modal analysis module. Here the relative values of the maximum, minimum and average stresses have been found. These are not the actual stress values. To know the actual values, a dynamic load must be applied to determine the stresses. For the 6 different modes, the different values of stresses are obtained.

CHAPTER 5

Simulation Results

Here, the results obtained from the simulation and experiment are presented and discussed. The results are presented sequentially. First, the mode shapes and natural frequencies of the 4-story structure is shown. Then the equivalent stresses are found. Also, the modal parameters for the different loading condition of the 4-story structure are shown.

5.1 Modal Analysis of 4-story Unloaded Structure

The natural frequency data for the unloaded and differently loaded 4-story structure is found from the modal analysis in ANSYS. From the simulation, the natural frequency of the first mode is 5.8371 Hz, and the sixth mode is 37.989 Hz. As the mode number increases so does the natural frequency. The mode shapes are also changing in the different axes. The first mode is bending in the Z axis. The second mode is bending in the X axis. A torsional or twisting mode can be seen in the Y axis. Rest of the modes are in the Z axis. A tabulated version of the modes is given in below.

Table 4: The first 6 modes and natural frequencies

Mode	Natural Frequency	Mode Shape
First Mode	5.8371 Hz	1st mode of bending in the Z axis
Second Mode	11.345 Hz	1st mode of bending in the X axis
Third Mode	12.392 Hz	1st mode of twisting in the Y axis
Fourth Mode	17.586 Hz	2nd mode of bending in the Z axis
Fifth Mode	29.017 Hz	3rd mode of bending in the Z axis
Sixth Mode	37.989 Hz	4th mode of bending in the Z axis

The 6 mode shapes of the 4-story structure are shown in Fig.11. These images have been taken from ANSYS. The bending and twisting modes can be seen from the figures. For the first mode, the structure is bending towards the Z axis with a natural frequency of 5.8371 Hz. The second mode a bending mode that is towards the X axis with a natural frequency of 11.345 Hz. The third mode is a twisting or torsional mode which is twisting in the Y axis of the structure. The natural frequency of this mode is 12.392 Hz. The 4th, 5th and 6th modes are bending modes in the Z axis. Here, different forms of bending can be seen. Here, nodes and anti-nodes are being created. The fourth mode has one node on the 2nd floor. This node indicates that there will be no displacement of this floor when the structure is excited to its natural frequency of 17.586 Hz. The anti-nodes in the other floors have the maximum displacement. So, when the structure reaches a natural frequency of 17.586 Hz, this phenomenon will occur. For the fifth mode, there are 2 modes created on the second and third floor so, there is no displacement in these two floors at the natural frequency of 29.017 Hz. The 4th floor has the maximum deflection since the anti-node is created at this floor. The sixth mode has 2 nodes at the natural frequency of 37.989 Hz. The mode shapes and natural frequency of the unloaded 4-story building can be seen in these figures below.

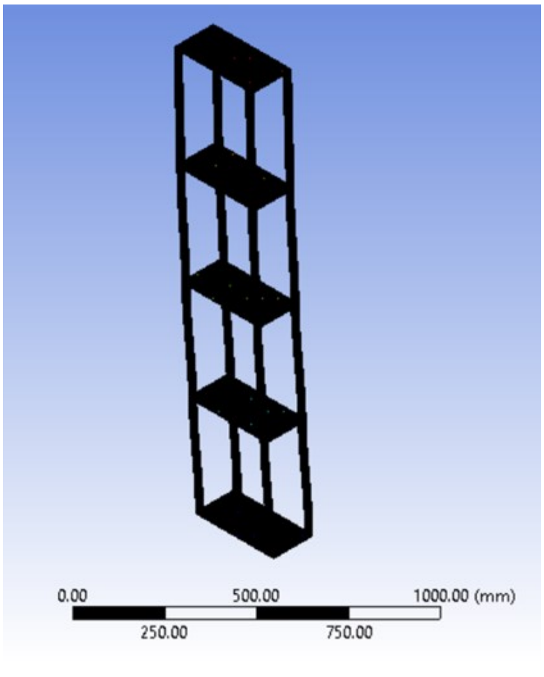

(a) Mode1: 5.8371 Hz Bending -Z axis

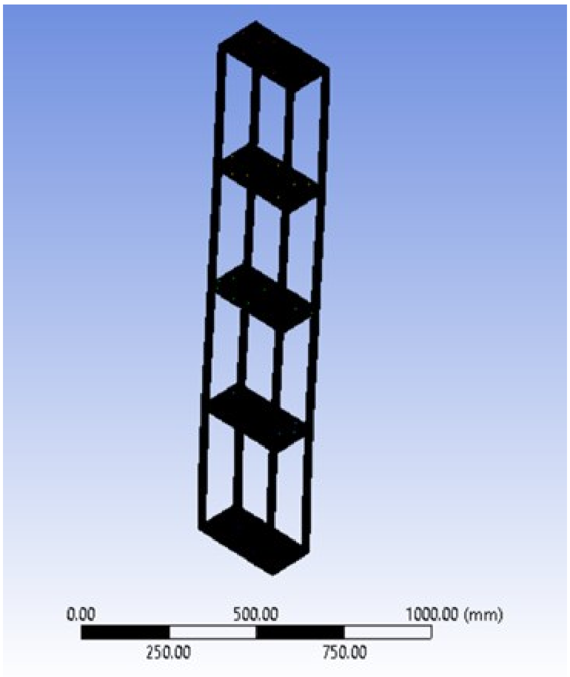

(b) Mode2: 11.345 Hz Bending -X axis

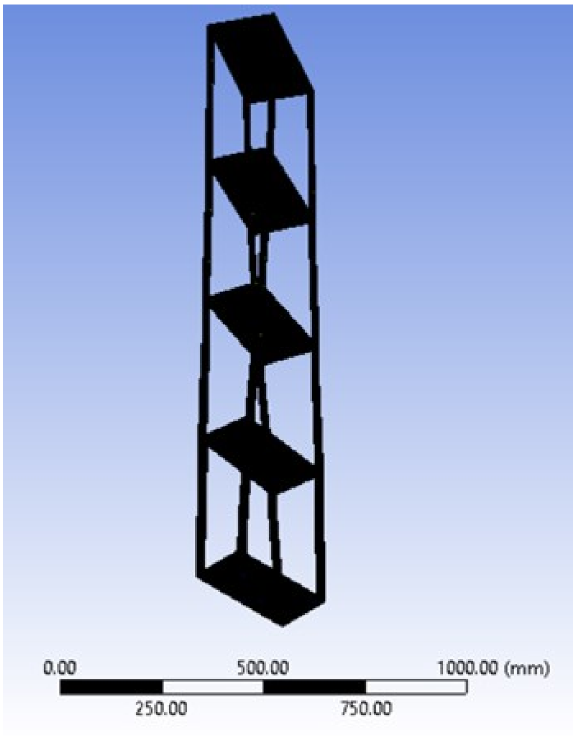

(c) Mode3: 12.392 Hz Twisting – Y axis

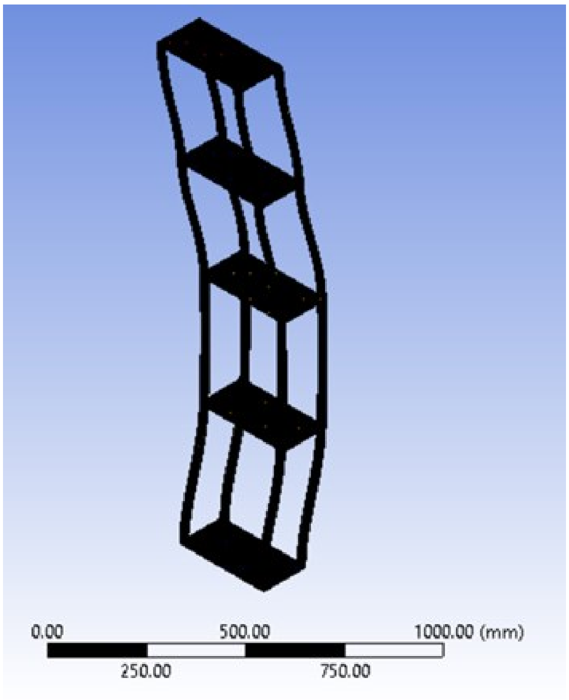

(d) Mode4: 17.586 Hz 2^{nd} Bending Z axis

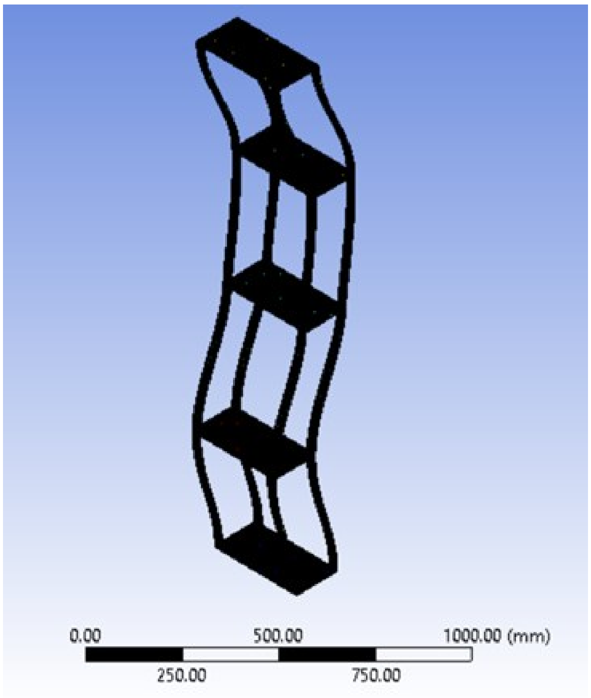

(e) Mode5: 29.017 Hz 3^{rd} Bending Z axis

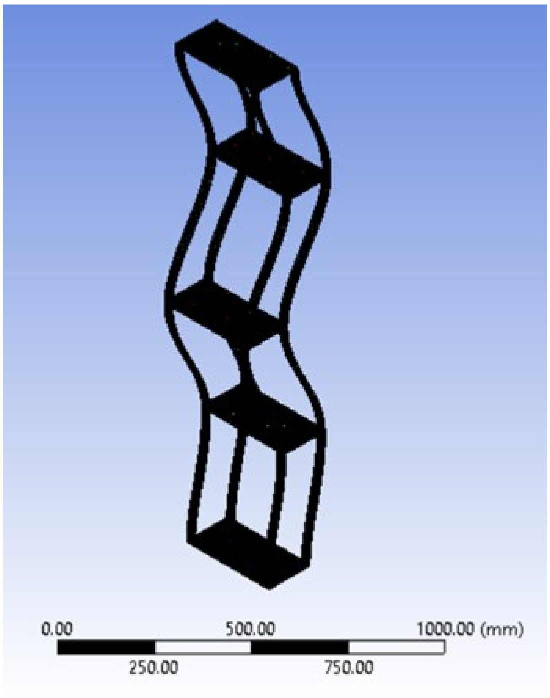

(f) Mode6: 37.989 Hz 4^{th} Bending Z axis

Figure 11: Extracted Six Mode Shapes of the Unloaded 4-story Structure.

5.2 Modal Analysis of the 4-story Loaded Structure

The natural frequency data for the loaded 4-story structure is found from the modal analysis in ANSYS. The tables here represent the modes and natural frequency of the loaded structure. There are several different configurations and each of them have a slight change in natural frequency. The loading has been done in 3 configurations. The loads have been placed in single floors, two floors and three floors.

Single floor loading refers to loads placed on only one floor while the other floors remain unloaded. The natural frequency data for single floor loading can be found in Table 5. When compared to the unloaded structure, the natural frequency increases gradually and for other instances, it has been seen to decrease or change in non-uniform ways. All the mode shape images are given in the appendix A1 for the reader to observe the change. For single floor loading conditions, the uniform change in natural frequency for bending vibration along the X axis and twisting mode about Y axis are observed. Interesting phenomena can be seen in the bending modes along the Z axis. For the 1st mode of bending along the Z axis, the natural frequency decreases as the load changes from one floor to another. But for the 2nd mode of bending along the Z axis, the natural frequency increases as the load are changed from one floor to another floor. A non-uniform change can be observed for the 3rd mode of bending. The change in natural frequency is not gradual as the load position is changed. Natural frequency increases when the load is on the second floor but decreases when it's placed on the 3rd floor. And when the load is on the 4th floor, the natural frequency increases with respect to the 3rd floor loading. For the 4th mode of bending, the natural frequency decreases when the load is on the 2nd floor. But gradually increases as the load position changes. It reaches a maximum value of 37.323 Hz when the load is on the 4th floor.

When any of the two floors are loaded at a time, natural frequency change can be seen in Table 6. When floors 1 and 2 are loaded, the natural frequency is 5.75 Hz along the Z axis for the 1st mode of bending. As the load position is changed from floors 1 and 3, the natural frequency decreases compared to floors 1 and 2 when they are loaded. This trend of decrease can be seen for the 1st mode of bending in the Z axis as the load position is changed. For the 2nd mode of bending, natural frequency is increasing and decreasing as the load position is changing. The natural frequency range for this condition is 16 Hz – 13 Hz. The 3rd mode of bending also exhibits a similar pattern with maximum and minimum natural frequency ranges to be 28 Hz – 22 Hz. This phenomenon continues into the 4th mode of bending along the Z axis.

A gradual decrease in natural frequency is seen for the bending along the X axis and twisting about the Y axis.

For the 3-floor loading condition, the natural frequency change can be observed in the Table 7. The gradual decrease of natural frequency for the 1st mode of bending along the Z axis. Similar pattern of the natural frequency continues into the 2nd mode of bending as well. For the 3rd mode of bending, no notable change of natural frequency can be seen but when the load is positioned in floors 1, 2 and 4, the natural frequency decreases compared to the other loading conditions. For the 4th mode of bending, the natural frequency increases with the change in load position. The natural frequencies decrease uniformly along the X axis and about the Y axis.

For better understanding, the reader may compare tables 4,5,6 and 7 together.

Table 5: Modes and Natural frequencies for single floor loading

1st floor load	Mode and frequency	2nd floor load	Mode and frequency	3rd floor load	Mode and frequency	4th floor load	Mode and frequency
1st mode of bending in the Z direction	6.0838 Hz	1st mode of bending in the Z direction	5.4747 Hz	1st mode of bending in the Z direction	4.9861 Hz	1st mode of bending in the Z direction	4.7095 Hz
2nd mode of bending in the Z direction	14.784 Hz	2nd mode of bending in the Z direction	15.714 Hz	2nd mode of bending in the Z direction	18.537 Hz	2nd mode of bending in the Z direction	15.442 Hz
3rd mode of bending in the Z direction	25.703 Hz	3rd mode of bending in the Z direction	28.874 Hz	3rd mode of bending in the Z direction	26.367 Hz	3rd mode of bending in the Z direction	27.272 Hz
4th mode of bending in the Z direction	37.017 Hz	4th mode of bending in the Z direction	34.471 Hz	4th mode of bending in the Z direction	35.116 Hz	4th mode of bending in the Z direction	37.323 Hz
1st mode of bending in the X direction	14.831 Hz	1st mode of bending in the X direction	14.947 Hz	1st mode of bending in the X direction	11.49 Hz	1st mode of bending in the X direction	9.6097 Hz
1st mode of twisting in the Y direction	14.83 Hz	1st mode of twisting in the Y direction	13.438 Hz	1st mode of twisting in the Y direction	11.666 Hz	1st mode of twisting in the Y direction	10.817 Hz

Table 6: Modes and Natural frequencies for double floor loading

1-2 floor load	Mode and frequency	1-3 floor load	Mode and frequency	1-4 floor load	Mode and frequency	2-3 floor load	Mode and frequency	2-4 floor load	Mode and frequency	3-4 floor load	Mode and frequency
1st mode of bending in the Z direction	5.7579 Hz	1st mode of bending in the Z direction	5.2418 Hz	1st mode of bending in the Z direction	4.93 Hz	1st mode of bending in the Z direction	4.8262 Hz	1st mode of bending in the Z direction	4.6217 Hz	1st mode of bending in the Z direction	4.2883 Hz
2nd mode of bending in the Z direction	14.569 Hz	2nd mode of bending in the Z direction	15.007 Hz	2nd mode of bending in the Z direction	13.407 Hz	2nd mode of bending in the Z direction	16.466 Hz	2nd mode of bending in the Z direction	13.083 Hz	2nd mode of bending in the Z direction	16.23 Hz
3rd mode of bending in the Z direction	22.529 Hz	3rd mode of bending in the Z direction	25.175 Hz	3rd mode of bending in the Z direction	23.498 Hz	3rd mode of bending in the Z direction	26.84 Hz	3rd mode of bending in the Z direction	28.175 Hz	3rd mode of bending in the Z direction	22.934 Hz
4th mode of bending in the Z direction	34.208 Hz	4th mode of bending in the Z direction	32.683 Hz	4th mode of bending in the Z direction	36.043 Hz	4th mode of bending in the Z direction	30.309 Hz	4th mode of bending in the Z direction	32.879 Hz	4th mode of bending in the Z direction	35.004 Hz
1st mode of bending in the X direction	19.611 Hz	1st mode of bending in the X direction	16.068 Hz	1st mode of bending in the X direction	12.53 Hz	1st mode of bending in the X direction	14.076 Hz	1st mode of bending in the X direction	12.852 Hz	1st mode of bending in the X direction	9.9766 Hz
1st mode of twisting in the Y direction	16.69 Hz	1st mode of twisting in the Y direction	14.255 Hz	1st mode of twisting in the Y direction	12.786 Hz	1st mode of twisting in the Y direction	12.691 Hz	1st mode of twisting in the Y direction	11.991 Hz	1st mode of twisting in the Y direction	10.537 Hz

Table 7: Modes and Natural frequencies for Triple floor loading

1-2-3 floor load	Mode and frequency	2-3-4 floor load	Mode and frequency	1-3-4 floor load	Mode and frequency	1-2-4 floor load	Mode and frequency
1st mode of bending in the Z direction	5.1084 Hz	1st mode of bending in the Z direction	4.2544 Hz	1st mode of bending in the Z direction	4.5162 Hz	1st mode of bending in the Z direction	4.8719 Hz
2nd mode of bending in the Z direction	14.851 Hz	2nd mode of bending in the Z direction	14.113 Hz	2nd mode of bending in the Z direction	13.995 Hz	2nd mode of bending in the Z direction	12.356 Hz
3rd mode of bending in the Z direction	23.015 Hz	3rd mode of bending in the Z direction	23.322 Hz	3rd mode of bending in the Z direction	20.652 Hz	3rd mode of bending in the Z direction	21.773 Hz
4th mode of bending in the Z direction	27.953 Hz	4th mode of bending in the Z direction	30.14 Hz	4th mode of bending in the Z direction	32.374 Hz	4th mode of bending in the Z direction	32.267 Hz
1st mode of bending in the X direction	19.893 Hz	1st mode of bending in the X direction	12.547 Hz	1st mode of bending in the X direction	13.8 Hz	1st mode of bending in the X direction	16.634 Hz
1st mode of twisting in the Y direction	16.091 Hz	1st mode of twisting in the Y direction	11.648 Hz	1st mode of twisting in the Y direction	12.788 Hz	1st mode of twisting in the Y direction	14.65 Hz

5.3 Stress Analysis of 4-story Unloaded Structure

The static stress developed in the structure has been found using the modal analysis. Here the relative stresses are presented. These do not indicate the actual stress values. The real stress values can be found through the application of loads. From the stress analysis, the stress regions mainly in the column and floor interface where the joint is present. The stresses then get transferred to the floors. For the 1st mode, the stress region is developed in the floor and column interface. For the twisting mode, the torsional stresses are being developed in the floors and columns. For the different modes of bending in the Z axis, the stress regions are developing in the anti-nodes where the displacement is the highest. These are in the columns while some of the stresses are being transferred to the floors. The table below shows the stress magnitude and the regions of stress.

Table 8: Stress analysis of unloaded 4-story structure

Mode	Frequency	Maximum Stress (MPa)	Minimum Stress (MPa)	Average Stress (MPa)	Stress Regions
1st	5.8371 Hz	151.37	1.5387e-13	11.921	Floor-column interface
2nd	11.345 Hz	362.54	1.137e-12	23.678	Floor-column interface with floor bending
3rd	12.392 Hz	175.19	1.1453e-12	30.78	Mostly in column and transferred to floors
4th	17.586 Hz	437.14	6.9438e-13	35.572	Floor-column interface node with least stress
5th	29.017 Hz	646.43	7.0308e-11	58.827	Floor-column interface node with least stress
6th	37.989 Hz	644	1.6271e-10	75	Mostly in column. Node with least stress

The figures represent the stresses developed in the different sections of the structure. The stresses are developing in the floor-column interfaces and the stresses are being transferred to the floors.

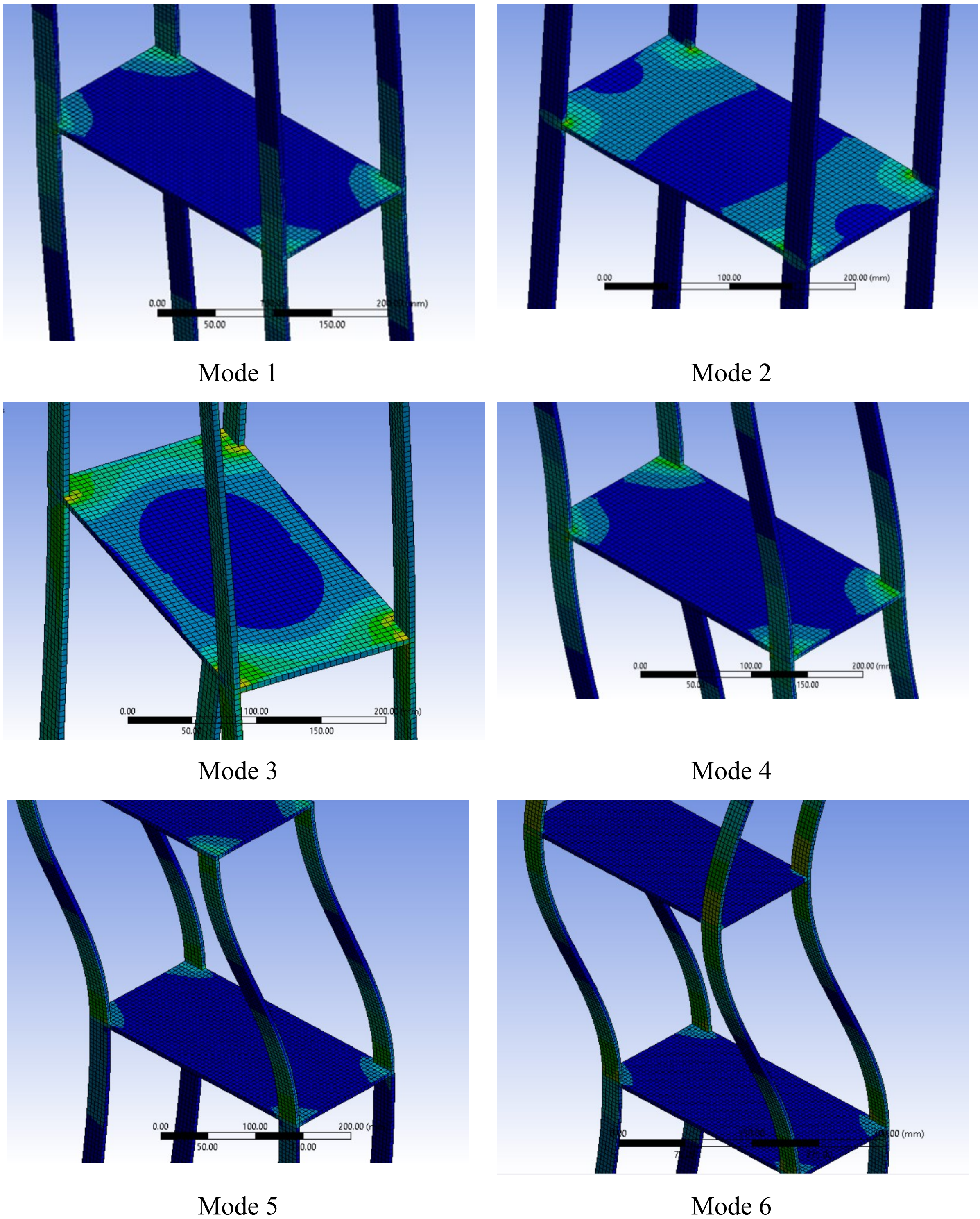

Figure 12: Stress analysis shows the regions where the maximum stresses develop during the bending and twisting modes.

CHAPTER 6
Validation

6.1 Experimentation

For validation of simulation results, it is necessary to conduct an experiment. A simple 2-story structure has been made and experimented with. The picture below represents the experimental model. The model has been fixed to the large base using wall bolts for a rigid fixing. The large base is used so that no disturbance is transferred to the structure during experiment.

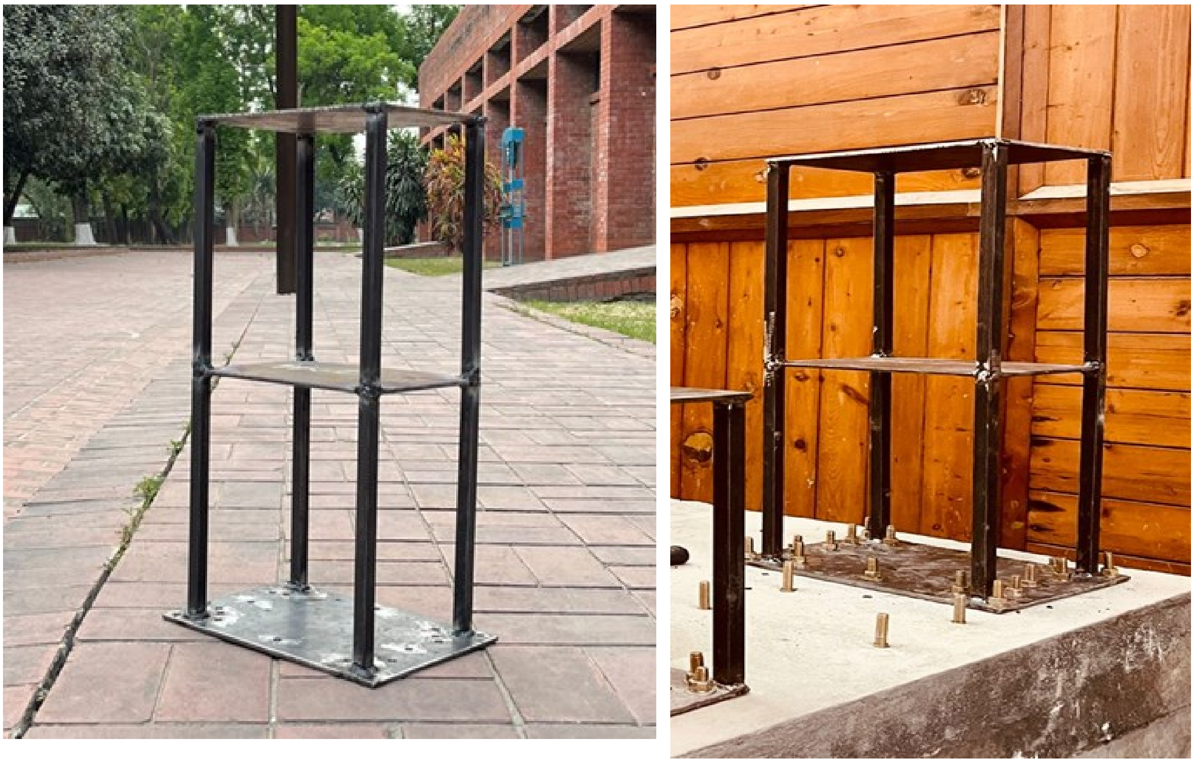

(a) 2-story structure (b) Structure attached to base

Figure 13: The 2-story experimental model attached to the base.

6.2 Model Design

For experimental purposes, a 2-story structure has been constructed. The structure is unloaded. It has been modelled in Solidworks 2017 and according to the design parameters, the experimental model has been made. The floors are 5 mm thick, and area is 254×177.8 mm^2. The floors are 254 mm high and with a cross-section of 15×15 mm^2. The base of the structure has been kept with some extra material for fixing purposes. It is 2 inches longer on the longer side and 1 inch longer on the wider side.

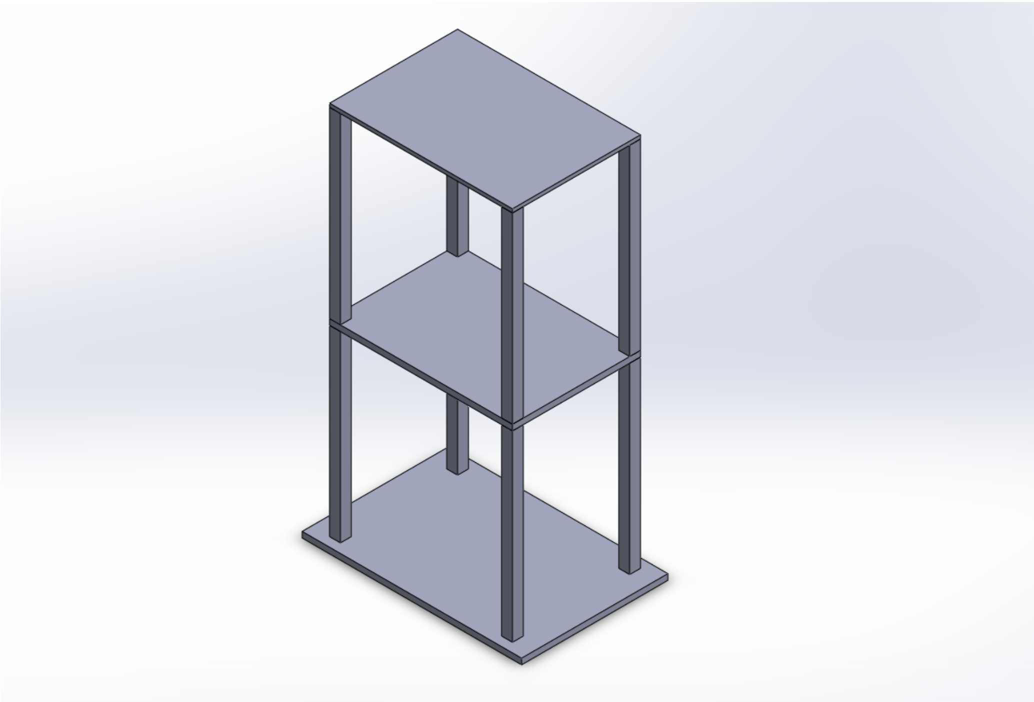

Figure 14: 2-story experimental model

The geometric parameters that have been used to construct the model is given in the table below.

Table 9: 2-story model geometric parameters.

Component	Length	Width	Height/thickness
Floor	254 mm	177.8 mm	5 mm
Column	15 mm	15 mm	254 mm
Total Height	523 mm		

Figure 15: Experimental Model

The material chosen for the experiment is mild steel since it is widely available and cost effective. The material properties are given in the table.

Table 10: 2-story model material properties

Material	Mild Steel		
Property	Symbol	Value	Unit
Density	P	8846	$Kg.m^{-3}$
Young's Modulus	E	1.9E+11	Pa
Poisson Ratio	υ	0.25	-
Bulk Modulus	K	1.2667E+11	Pa
Shear Modulus	G	7.6E+10	Pa
Thermal Expansion coefficient	A	1.2E-05	C^{-1}

(a) Columns cut to size

(b) Plates cut to size

(a) Final structure fixed to base

Figure 16: 2-story model

6.3 Experimental Setup

For experimentation, vibration measurement instruments have been used. All these instruments have been available in the laboratory. The instrument list contains the electrodynamic vibration shaker, load and displacement sensors, oscilloscope, and frequency generator. They have been kept at a controlled environment to protect them from humidity, solar radiation, and other environmental components.

The table below holds the information such as model number and name of each instrument and their use cases.

Table 11: Instruments used and their model numbers

Instrument	Model Number	Use
Oscilloscope	GW-Instek GDS – 1102B	2 channel, digital storage oscilloscope
Function Generator	Texio FG-281	Function generator
Electrodynamic Vibration Shaker	MTS 2075E	75lbf dual purpose shaker
Power Amplifier	SmartAmp 2100E21	Solid-state amplifier
Eddy current displacement sensor	-	Sensing displacement

These instruments have been used to provide input and tabulate the output. For modal testing, the electrodynamic vibration shaker has been used to provide a steady sinusoidal force. The eddy current displacement sensor allows for the measurement of the displacement caused in the building. The function generator supplied a steady frequency input of sinewaves. And finally, the oscilloscope allowed for the measurement of output data.

For the experiment, a complete setup has been made consisting of the electrodynamic vibration shaker, load sensors, displacement sensors, oscilloscope, frequency generator, amplifier, power supply and laptop for data collection. The electrodynamic vibration shaker has been fixed to the concrete base using wall bolts to fasten it securely. The load sensor is placed on the arm of the vibration shaker. An output wire comes out from the load sensor, and it connects to the oscilloscope. The load sensor measures the amount of load being imparted by the shaker to the structure. The eddy current displacement sensor is placed on a stand and fixed securely. The output wire from the sensor is taken to the oscilloscope. This way the output is measured. Inputs are given to the shaker through the frequency generator.

Figure 17: Setup for performing the experiment.

The electrodynamic shaker or excitor has been attached to one of the legs of the structure. A load sensor is attached to the shaker input arm. The displacement sensor has been set to the top of the structure to measure movements.

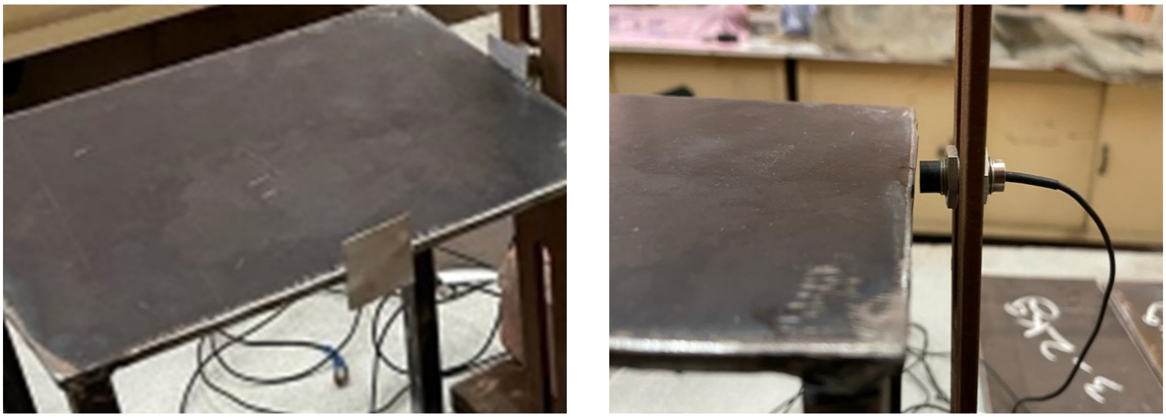

(a) Aluminum strip for sensor (b) Sensor arrangement

Figure 18: Eddy current displacement sensor setup

The oscilloscope and frequency generator has been setup in this arrangement. The frequency generator provides with the desired input signal to the dynamic shaker and the data is collected from the oscilloscope. Finally, the data has been collected in Excel for graphical analysis.

Figure 19: Oscilloscope and frequency generator setup.

The laboratory environment has been kept under control. No external sources of noise and vibration have been present during experimentation. A constant power supply has been provided for the instruments.

Figure 20: Laboratory setup

6.4 Simulation of 2-story Building and Comparison with Experimental Results

For the experiment, a simulation has been performed on the 2-story unloaded model. The simulation results are then validated using the experimental data.

The modal analysis to find the natural frequencies of the 2-story model has been done. In ANSYS, the modal analysis has been performed by meshing the 2-story structure and giving it boundary conditions. The first table shows the mesh results of the structure. The next table shows the natural frequency of the first 6 modes extracted.

Table 12: Mesh data generated for the 2-story structure

Settings	Description
Physics Preference	ANSYS Mechanical
Element Type	Rectangular
Element Order	Program Controlled
Element Size	5-millimeters
Number of Nodes	85687
Number of Elements	14182

Table 13: Mode shape and Natural Frequency of 2-story Structure

Mode	Natural Frequency
1st	46.766 Hz
2nd	50.302 Hz
3rd	78.608 Hz
4th	144.24 Hz
5th	148.26 Hz
6th	231.36 Hz

The natural frequency has been found through harmonic response analysis method. In this method, the electrodynamic vibration shaker applied constant sinusoidal load to the desired location. The load has been applied to the right column of the building when it is viewed towards the point of application. The displacement value from the eddy current displacement sensor has been measured and used to find the frequency response by dividing and normalizing it using the input force value. The displacement and force values have been converted to voltage values using the conversion factors provided by the instrument manufacturers.

Here, the experimental and simulation results are shown. A harmonic analysis has been done in the simulation to show the 1st and 5th mode of the 2-story structure during excitation. In the experiment, the data has been plotted. From the plot, the peaks of mode 1 and 5 have been found. By comparing these two results, the percentage of error is found for the modes 1 and 5 are 6.23 and 3.87 percent. This concludes the validity of the simulation results.

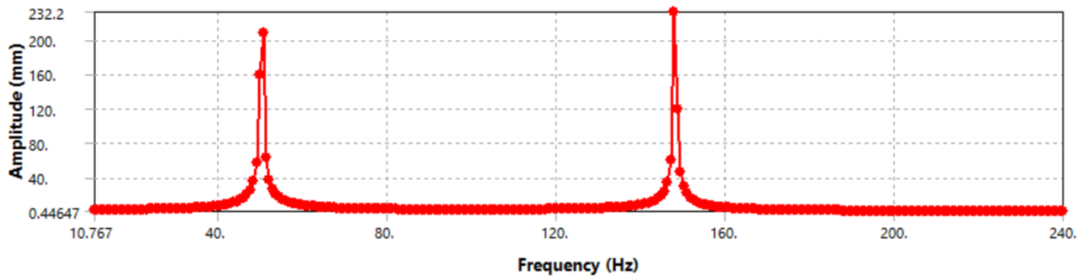

Figure 21: FRA results obtained from ANSYS. The graph is linear. The two peaks indicate the natural frequencies of mode-1 and mode-5.

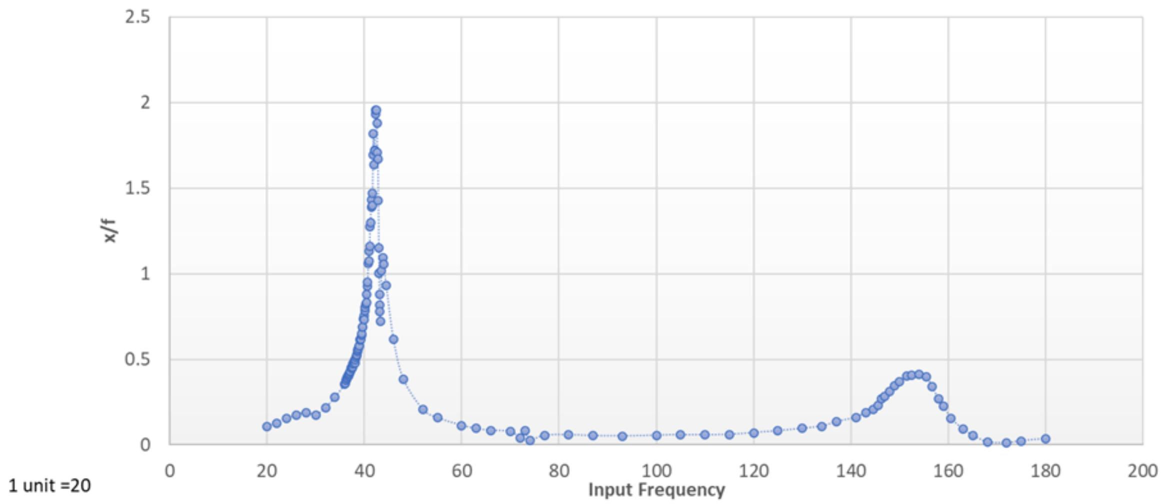

Figure 22: The FRA result for the experimental validation.

Thus, the simulation results have been validated through experiment. Figure 22 represents the experiment which is closely matching with the simulation in figure 21.

CHAPTER 7

Discussion on Results

Simulations for the modal analysis and stress analysis have been done for the 4-storied structures.

The modal analysis of the unloaded and loaded 4-storied structures have been performed. The mode shapes and natural frequencies for both structures have been found. For the unloaded 4-story structure, the natural frequencies range from 5.8371 Hz to 37.989 Hz along the different bending and twisting modes. The mode shapes are found along X, Y and Z axes. The mode shape types are bending and twisting. The twisting mode is about the Y axis. The bending modes are along the Z and X axis. The Z axis displays 3 modes of bending. In these modes of bending, nodes are created in different floor levels. These nodes indicate that there is no displacement of the floors when the structure is vibrating in its natural frequency. The anti-nodes are created in other floor levels. These anti-nodes represent the maximum displacement of the floors when the structure is vibrating at the natural frequency.

For the loaded 4-story structure, the change in natural frequency can be seen. The loading has been done in single floor, double floor, and triple floor combinations. For the 3 loading cases, the natural frequency for bending mode in the X axis and twisting mode in Y axis decrease gradually as the load height changes. For the natural frequencies in the Z axis, the change is not uniform. The natural frequencies are either increasing when the loads are changing position, or it is changing in a periodic manner. First the mode is decreasing, then it is increasing and again it is decreasing. This change is due to the change in the position of the load. The reason for this change in natural frequencies can be interpreted by considering mass and stiffness of the structure. For single floor loading, as the load is being transferred from one floor to another floor, the natural frequency decreases for some cases. This may be due to higher mass in the lower floors causing higher natural frequency and higher stiffness for upper floor loading cases causing lower natural frequencies. For double floor loading and triple floor loading cases, the loading combinations alter the mass and stiffness matrices of the structure and thus causing this phenomenon in the natural frequency.

Stress analysis has been done for the unloaded 4-storied structure. The analysis shows the Von Mises stress developed from the 6 modes that have been extracted. The stress regions are mainly in the floor-column interface. These regions have the highest stresses. The stress regions vary for the different modes. For the 2nd mode, the stresses are being transferred from the floor-column interface to the floors. For the 6th mode, the stresses are developing in the columns. The maximum stress levels are ranging from 151.37 Hz for the 1st mode to 644 Hz for the 6th mode.

From the experiment, the validation of the simulation results has been done for the 2-story model. The natural frequencies and mode shapes of the 2-story structure have been found through simulation. For validating the results, an experiment has been performed. The experiment has been done using a real 2-story model that has been excited using an electrodynamic shaker. The harmonic response of the structure has been plotted and this result matches to the frequency response analysis that has been performed in the simulation. The harmonic response of the model building indicates two natural frequencies. these are modes 1 and 5 and their corresponding natural frequency of 43.2 Hz and 144.6 Hz. These results are very close to the simulation. This concludes the validation.

Conclusion

So, in conclusion we can say that we have found the modal parameters of the 4-story structure, both loaded and unloaded conditions, and validated the results experimentally using a 2-story model structure. We have seen the development of relative stresses in the unloaded 4-story structure.

To comment on the natural frequency of the unloaded and differently loaded structures, it can be said that the change in the frequency is happening due to the change in loading conditions. For the unloaded structure, the frequency values are seen to change with the mode numbers. But for the loaded conditions, things are different. The natural frequency values are not uniformly changing for the different Z-axis bending cases. For some cases, it is increasing gradually while for others, it is changing non-uniformly. This is due to the various loading combinations and the amount of loading. This is also causing different mode shapes as well. Here, nodes with zero deflection and anti-nodes with the maximum deflection is being created. These are important phenomena that need to be well understood.

From the stress analysis, the relative stresses have been found. Even though they are not actual values, they do identify the maximum stress regions.

The experiment allowed for verifying the simulation result. From the experiment, the FRA has been determined and the simulation matches this. The experimental setup also laid the foundation for further studies that are needed to be done.

Without performing rigorous mathematical calculations analytically, the use of numerical and experimental methods can produce accurate results. Therefore, one can rely on numerical methods to reliably design and analyze the modal characteristics of a structure without the need of expensive experiments.

Limitations

Like all research, there are some limitations to this study. The one that slowed down the progress of this research is the limitation of time. As the world recovered from the pangs of the COVID-19 pandemic, academia went through a bumpy start.

- The stress analysis of the unloaded 4-storied structure has been done to find the relative stresses. Since no dynamic loading has been applied, the actual stresses have not been studied. The stress characteristics of the loaded 4-storied structure has not been done. Also, the validation of the stress data has not been done through experimentation.
- The effects of the torsional modes have not been studied since the research focused on the lateral and longitudinal forces only.
- The structure has not been excited with actual seismic loading conditions. To understand the dynamic behavior of the structure, it is important.
- The structure-foundation interaction has not been studied.
- The sources of non-linearity within the structure have not been investigated.
- The effect of other types of loadings, such as point loads, have not been studied.
- Wind load, gravity load, ambient vibrations and various other loading conditions have not been incorporated into the study to understand the dynamic behavior of the structure.

Future Scope

The future scopes of this study are:

- Carry out modal analysis on 10 storied structures.
- See the effect of seismic loading through harmonic analysis by applying real data to the system and evaluating for that.
- Investigate on the dynamic stresses on the structure for both loaded and unloaded structure.
- Perform fatigue analysis.
- Understand the effects of different types of loading on the structure.
- Compare the characteristics of a healthy structure to a structure with defects.
- See the effects of wind loads, gravity loads, ambient vibration, human interaction etc. on the structure.
- Observe the effects of different materials on the dynamic behavior of the structure.
- Incorporate vibration control systems to mitigate the excitation forces affecting the structure.
- Introduce machine learning, computer vision, artificial intelligence, IoT sensors to advance the research into higher grounds.

References

[1] C. Eng, "Structural vibration analysis: Modelling, analysis and damping of vibration structures," *Eng. Anal.*, vol. 1, no. 1, p. 63, 1984, doi: 10.1016/0264-682x(84)90015-7.

[2] M. L. Chandravanshi and A. K. Mukhopadhyay, "Modal analysis of structural vibration," *ASME Int. Mech. Eng. Congr. Expo. Proc.*, vol. 14, pp. 1–9, 2013, doi: 10.1115/IMECE2013-62533.

[3] C.-M. Uang and M. Bruneau, "State-of-the-Art Review on Seismic Design of Steel Structures," *J. Struct. Eng.*, vol. 144, no. 4, p. 03118002, 2018, doi: 10.1061/(asce)st.1943-541x.0001973.

[4] T. V. Galambos, "Recent research and design developments in steel and composite steel-concrete structures in USA," *J. Constr. Steel Res.*, vol. 55, no. 1–3, pp. 289–303, 2000, doi: 10.1016/S0143-974X(99)00090-5.

[5] K. Ghaedi, Z. Ibrahim, H. Adeli, and A. Javanmardi, "Invited review: Recent developments in vibration control of building and bridge structures," *J. Vibroengineering*, vol. 19, no. 5, pp. 3564–3580, 2017, doi: 10.21595/jve.2017.18900.

[6] G. Song, V. Sethi, and H. N. Li, "Vibration control of civil structures using piezoceramic smart materials: A review," *Eng. Struct.*, vol. 28, no. 11, pp. 1513–1524, 2006, doi: 10.1016/j.engstruct.2006.02.002.

[7] K. Roik, U. Dorka, and P. Dechent, "Vibration control of structures under earthquake loading by three-stage friction-grip elements," *Earthq. Eng. Struct. Dyn.*, vol. 16, no. 4, pp. 501–521, 1988, doi: 10.1002/eqe.4290160404.

[8] O. El-Khoury and H. Adeli, "Recent Advances on Vibration Control of Structures Under Dynamic Loading," *Arch. Comput. Methods Eng.*, vol. 20, no. 4, pp. 353–360, 2013, doi: 10.1007/s11831-013-9088-2.

[9] Bhave Shrikant, *Mechanical Vibrations: Theory and Practice*, 1st ed. New Delhi: Pearson India, 2010.

[10] X. Wang, "Analysis of a Single Degree of Freedom Spring-Mass-Dashpot System Using Transfer Function, Integration, State Space, and Frequency Response Methods," *Freq. Anal. Vib. Energy Harvest. Syst.*, pp. 1–13, 2016, doi: 10.1016/b978-0-12-802321-

1.00001-7.

[11] R. W. C. BAHRAM NOUR-OMID, "Short communication," *Earthq. Eng. Struct. Dyn.*, vol. 13, pp. 271–275, 1985, doi: https://doi.org/10.1002/eqe.4290130210.

[12] SIMSCALE, "What is von Mises Stress?," 2021. https://www.simscale.com/docs/simwiki/fea-finite-element-analysis/what-is-von-mises-stress/ (accessed May 09, 2022).

[13] S. L. Chan, "Vibration and modal analysis of steel frames with semi-rigid connections," *Eng. Struct.*, vol. 16, no. 1, pp. 25–31, 1994, doi: 10.1016/0141-0296(94)90101-5.

[14] B. Vivek and P. Raychowdhury, "Experimental modal analysis of a steel frame structure with SFSI effects," no. November, 2015.

[15] Y. Zhou, A. Kareem, and M. Gu, "Mode Shape Corrections for Wind Load Effects," *J. Eng. Mech.*, vol. 128, no. 1, pp. 15–23, 2002, doi: 10.1061/(asce)0733-9399(2002)128:1(15).

[16] Y. Zhou and A. Kareem, "Torsional load effects on buildings under wind," *Struct. Congr. 2000 Adv. Technol. Struct. Eng.*, vol. 103, 2004, doi: 10.1061/40492(2000)84.

[17] S. Sandun De Silva and D. P. Thambiratnam, "Dynamic characteristics of steel-deck composite floors under human-induced loads," *Comput. Struct.*, vol. 87, no. 17–18, pp. 1067–1076, 2009, doi: 10.1016/j.compstruc.2009.04.005.

[18] Y. Kwak, S. Lee, J. Park, D. Hwang, J. Y. Jeon, and J. Park, "Effect of the static compressive load on vibration propagation in multistory buildings and resulting heavyweight floor impact sounds," *J. Acoust. Soc. Am.*, vol. 142, no. 1, pp. 308–316, 2017, doi: 10.1121/1.4994290.

[19] C. M. Chan and J. K. L. Chui, "Wind-induced response and serviceability design optimization of tall steel buildings," *Eng. Struct.*, vol. 28, no. 4, pp. 503–513, 2006, doi: 10.1016/j.engstruct.2005.09.005.

[20] K. T. Tse, P. A. Hitchcock, and K. C. S. Kwok, "Mode shape linearization for HFBB analysis of wind-excited complex tall buildings," *Eng. Struct.*, vol. 31, no. 3, pp. 675–685, 2009, doi: 10.1016/j.engstruct.2008.11.012.

[21] T. ting Ma, L. Zhao, N. yu Chen, Y. jun Ge, and D. Zhang, "Wind-induced dynamic

performance of a super-large hyperbolic steel-truss cooling tower," *Thin-Walled Struct.*, vol. 157, no. January, p. 107061, 2020, doi: 10.1016/j.tws.2020.107061.

[22] X. Chen and A. Kareem, "Coupled Dynamic Analysis and Equivalent Static Wind Loads on Buildings with Three-Dimensional Modes," *J. Struct. Eng.*, vol. 131, no. 7, pp. 1071–1082, 2005, doi: 10.1061/(asce)0733-9445(2005)131:7(1071).

[23] X. Chen and A. Kareem, "Equivalent Static Wind Loads on Buildings: New Model," *J. Struct. Eng.*, vol. 130, no. 10, pp. 1425–1435, 2004, doi: 10.1061/(asce)0733-9445(2004)130:10(1425).

[24] M. Sahin and M. Ozturk, "Uniform Shear Buildings under the Effect of Gravity Loads," *J. Eng. Mech.*, vol. 133, no. 1, pp. 48–57, 2007, doi: 10.1061/(asce)0733-9399(2007)133:1(48).

[25] D. Bernal, "Instability of Buildings Subjected to Earthquakes," *J. Struct. Eng.*, vol. 118, no. 8, pp. 2239–2260, 1992, doi: 10.1061/(asce)0733-9445(1992)118:8(2239).

[26] "effect of gravity loading on the earthquake response of cooling towers.pdf." .

[27] MATWEB, "Mild Steel Standard Data." https://www.matweb.com/search/datasheet.aspx?bassnum=MS0001&ckck=1 (accessed May 09, 2022).

[28] Texio, "FG-281 Function Generator - Discontinued - Product detail | TEXIO TECHNOLOGY CORPORATION_.pdf." https://www.texio.co.jp/en/product/detail/22.

[29] GW INSKTEK, "Instek GDS-1102B 100MHz , 2-Channel , 1Gs / S , Digital Storage Oscilloscope," 2008. https://www.signaltestinc.com/product-p/gds-1102b.htm.

[30] The Modal Shop INC., "SmartAmp ™ Power Amplifier Product Manual." https://www.modalshop.com/excitation/SmartAmp-Power-Amplifier?ID=357.

[31] The Modal Shop INC., "75 lbf Dual Purpose Shaker." https://www.modalshop.com/excitation/75-lbf-Dual-Purpose-Shaker?ID=251.

[32] Panasonic, "Eddy Current Type Displacement Sensor - Displacement Sensors | Technical Guide - Panasonic Eddy Current Type Displacement Sensor - Displacement Sensors."

https://www3.panasonic.biz/ac/ae/service/tech_support/fasys/tech_guide/measurement/eddy_current_type/index.jsp.

Appendix

A.1 Mode Shapes and Natural Frequencies of Loaded Structures

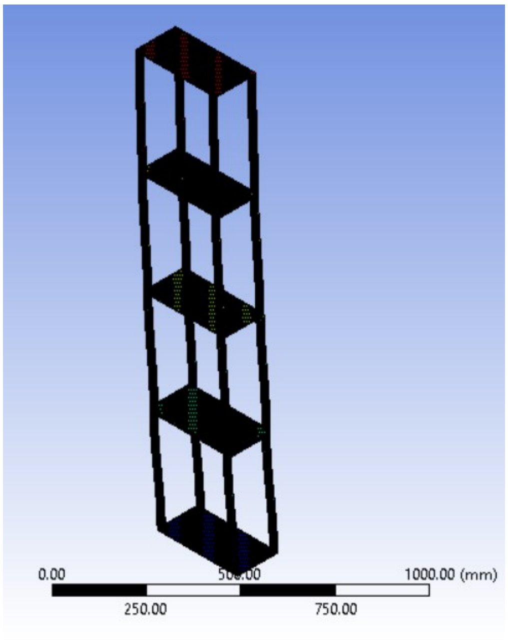

(a) Mode 1 - 6.0838 Hz

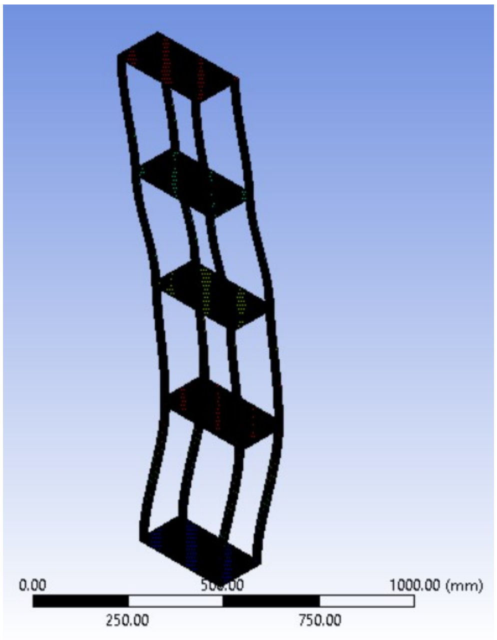

(b) Mode 2 - 14.784 Hz

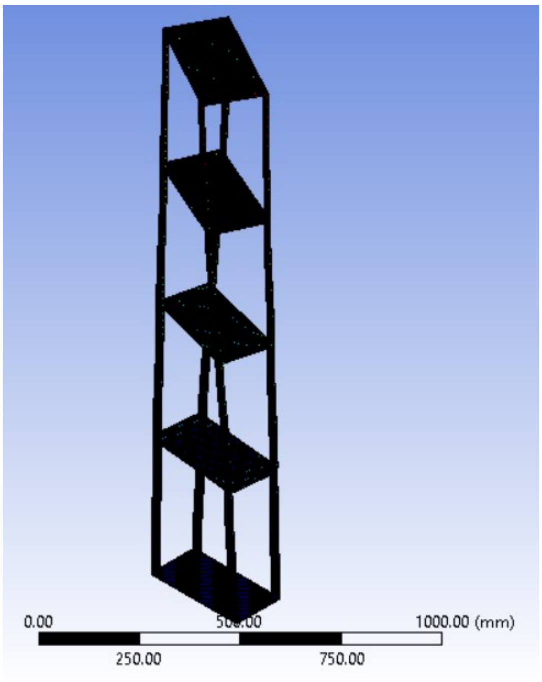

(c) Mode 3 - 14.83 Hz

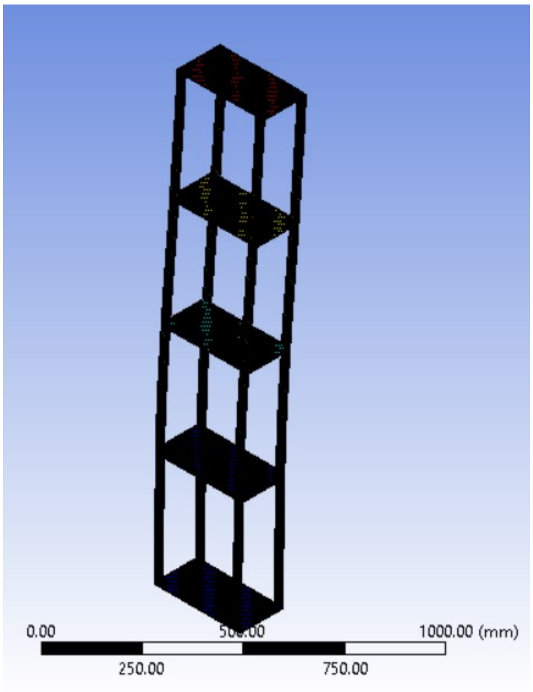

(d) Mode 4 - 14.831 Hz

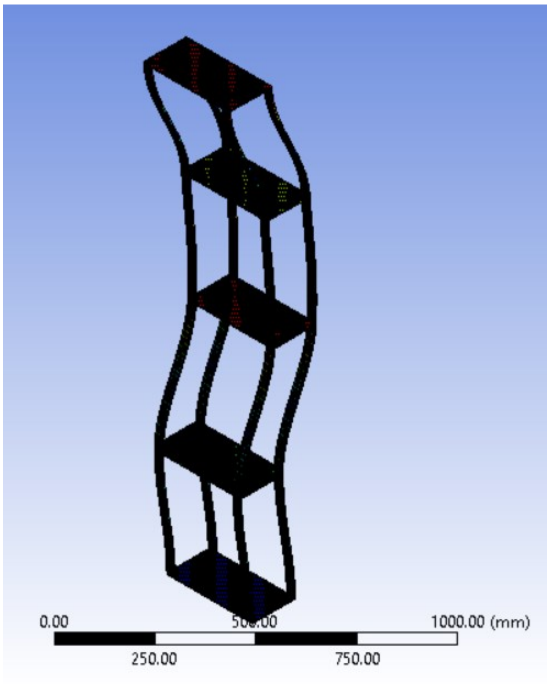

(e) Mode 5 - 25.703 Hz

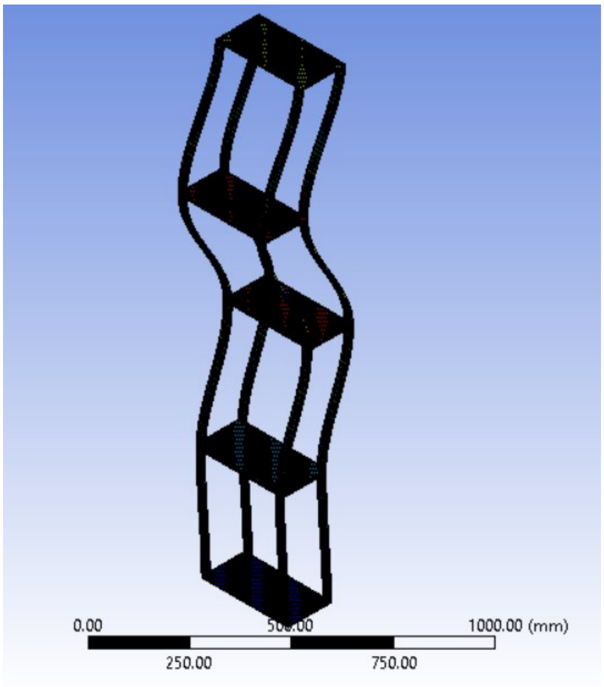

(f) Mode 6 - 37.017 Hz

Figure 23: Mode shapes and natural frequency when only 1st floor is loaded with UDL.

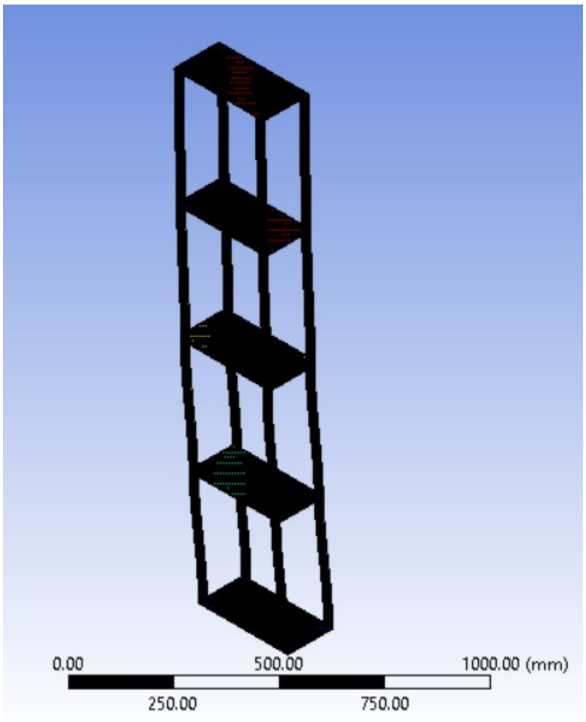

(a) Mode 1 - 5.4747 Hz

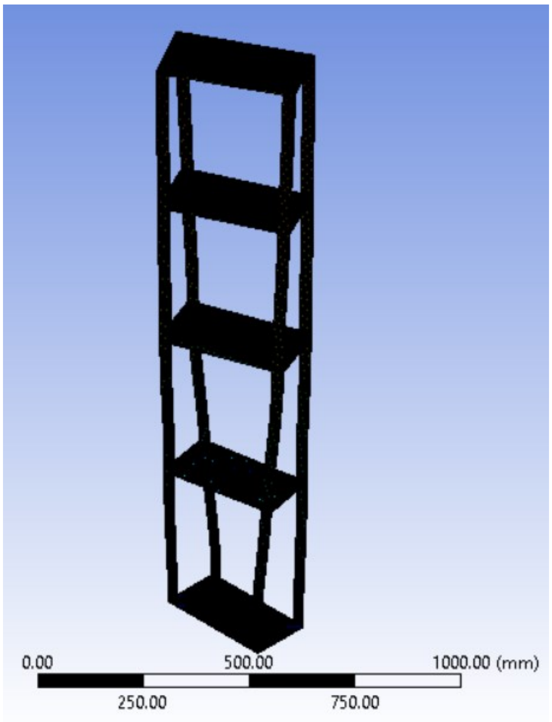

(b) Mode 2 - 13.438 Hz

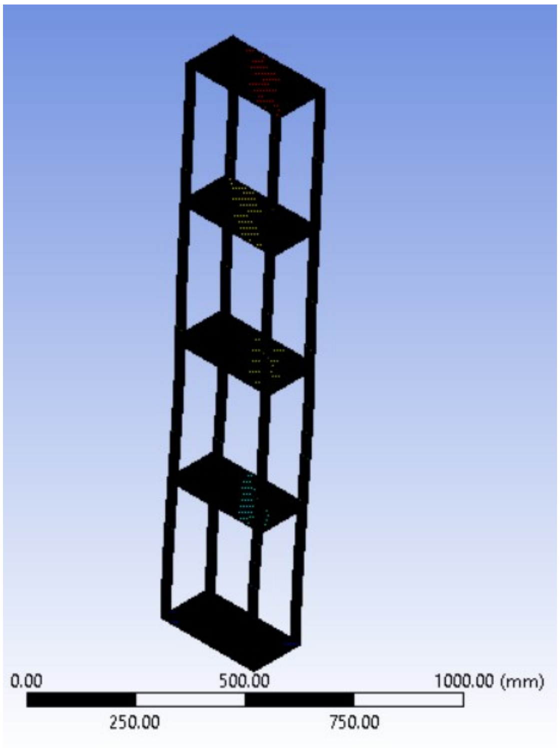

(c) Mode 3 - 14.947 Hz

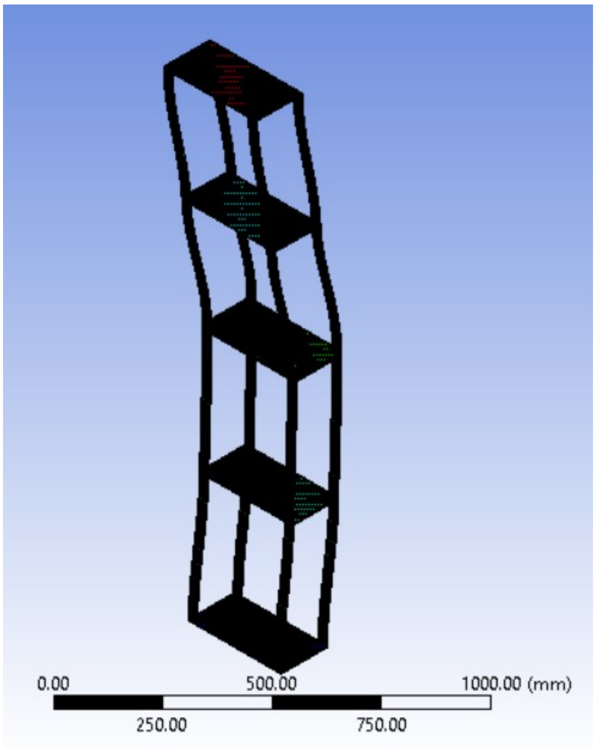

(d) Mode 4 - 15.714 Hz

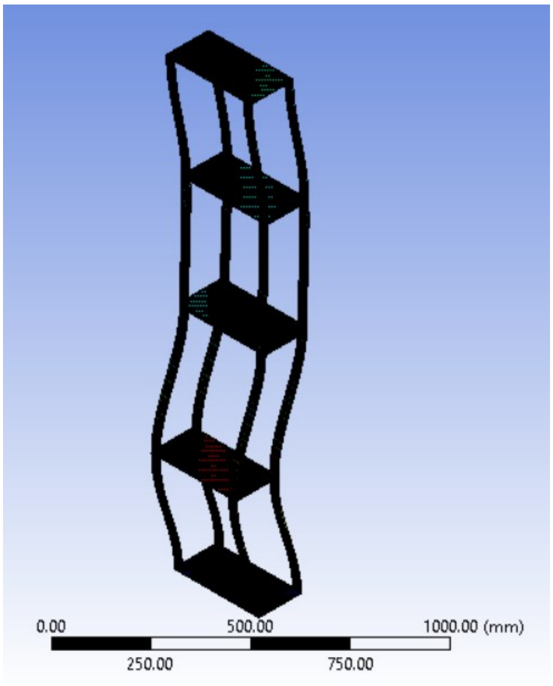

(e) Mode 5 - 28.874 Hz

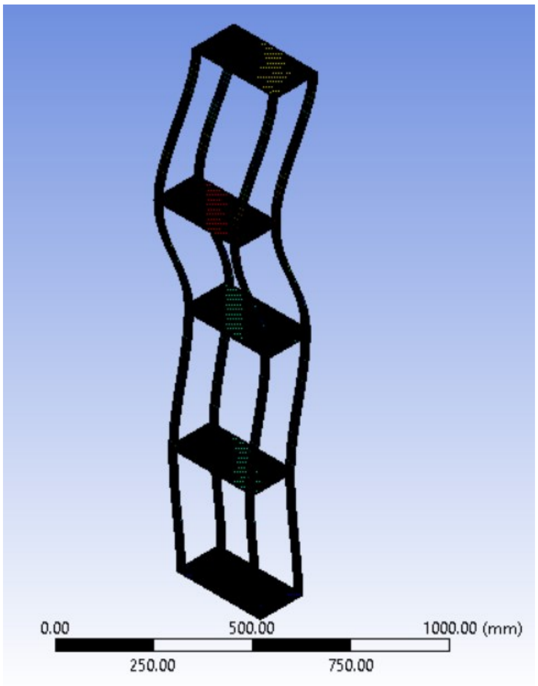

(f) Mode 6 - 34.471 Hz

Figure 24: Mode shapes and natural frequency when only 2nd floor is loaded with UDL.

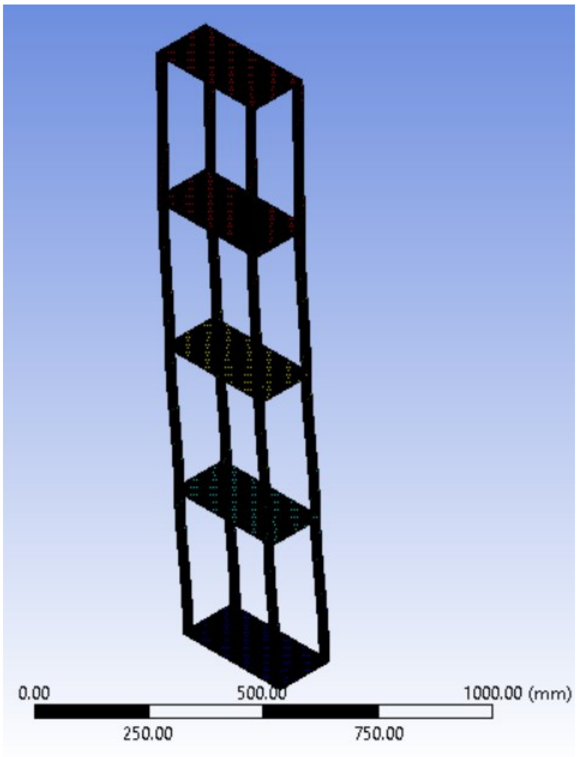

(a) Mode 1 - 4.9861 Hz

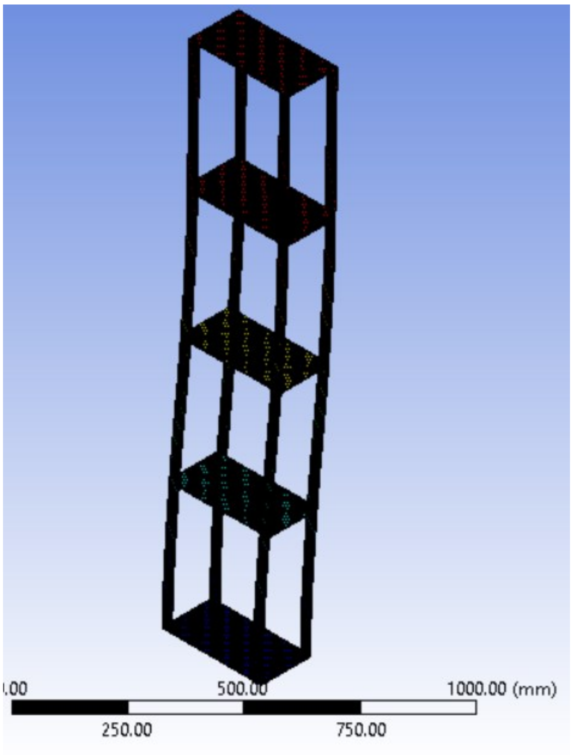

(b) Mode 2 - 11.49 Hz

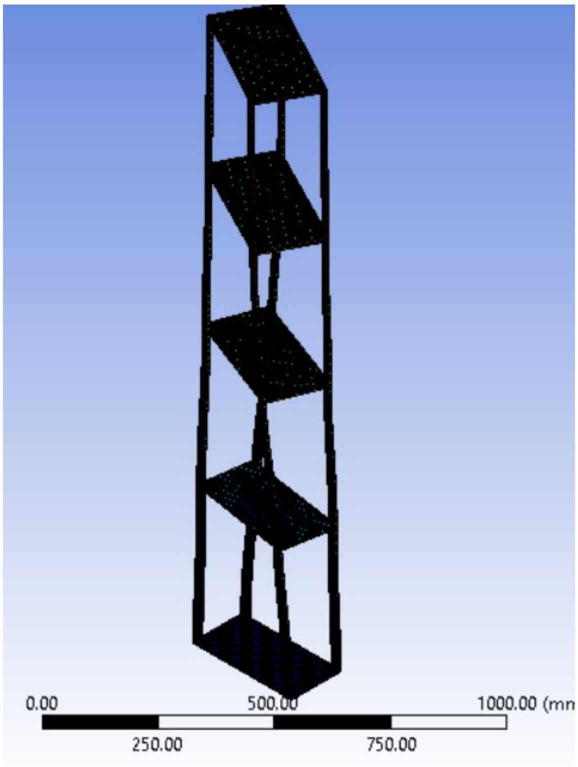

(c) Mode 3 - 11.666 Hz

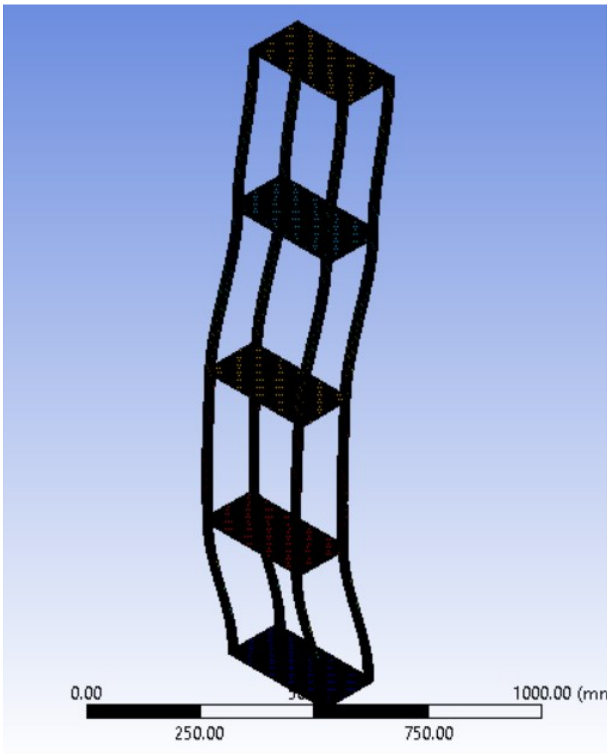

(d) Mode 4 - 18.537 Hz

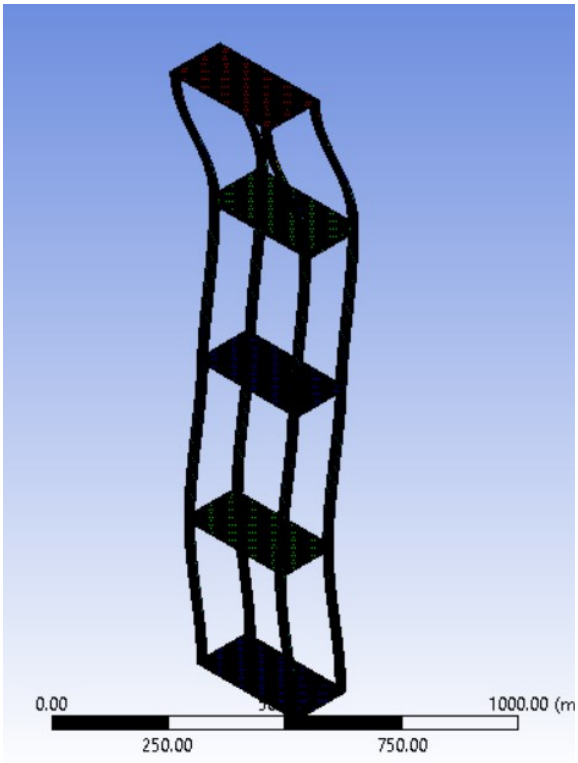

(e) Mode 5 - 26.367 Hz

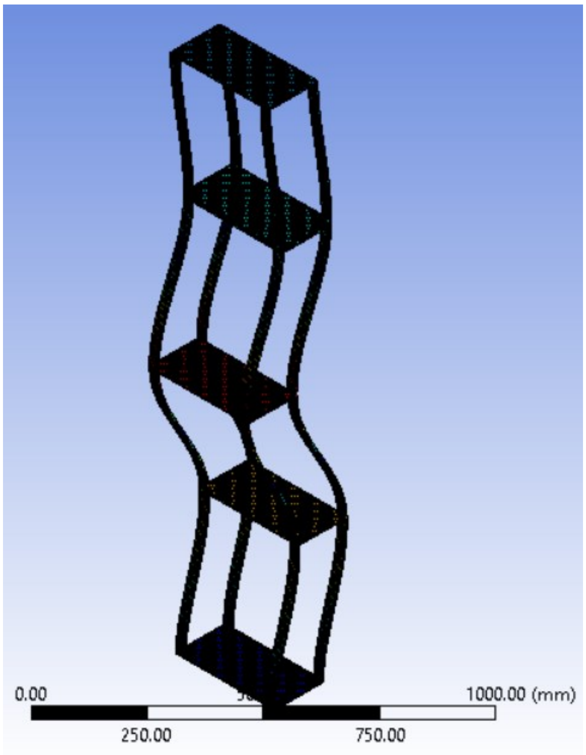

(f) Mode 6 - 35.116 Hz

Figure 25: Mode shapes and natural frequency when only 3rd floor is loaded with UDL.

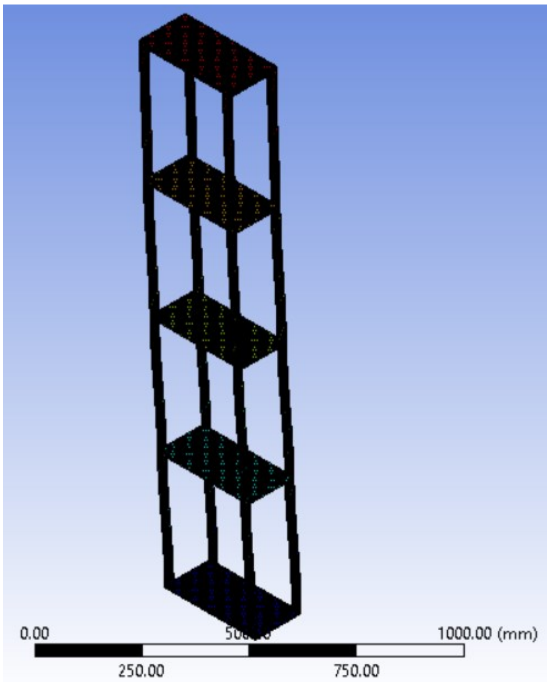

(a) Mode 1 - 4.7095 Hz

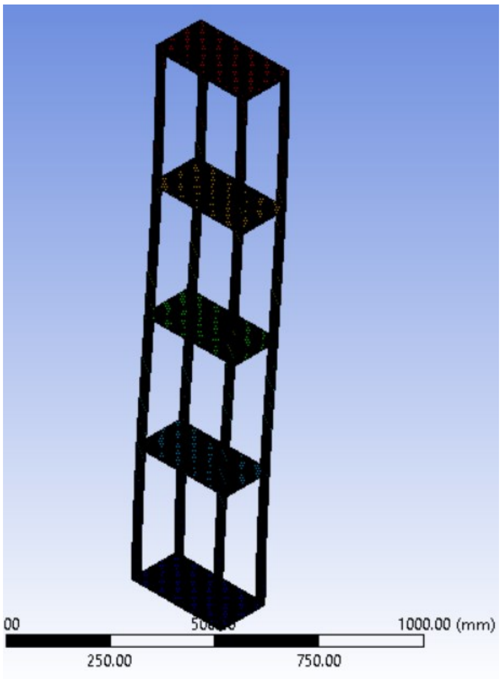

(b) Mode 2 - 9.6097 Hz

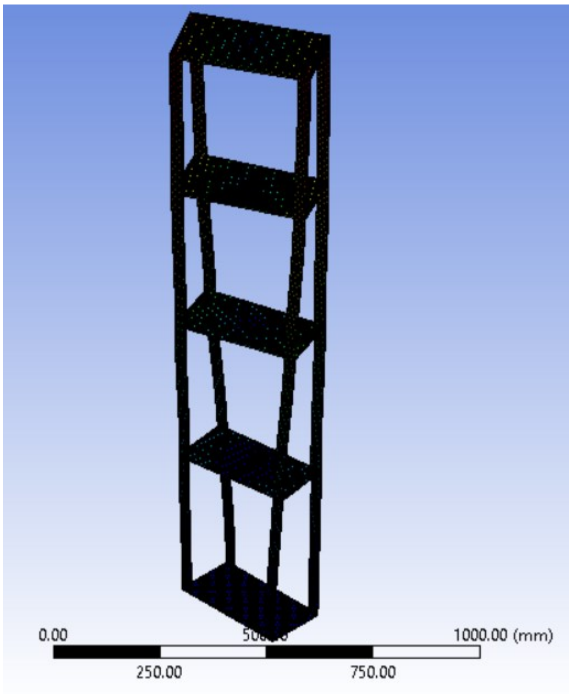

(c) Mode 3 - 10.817 Hz

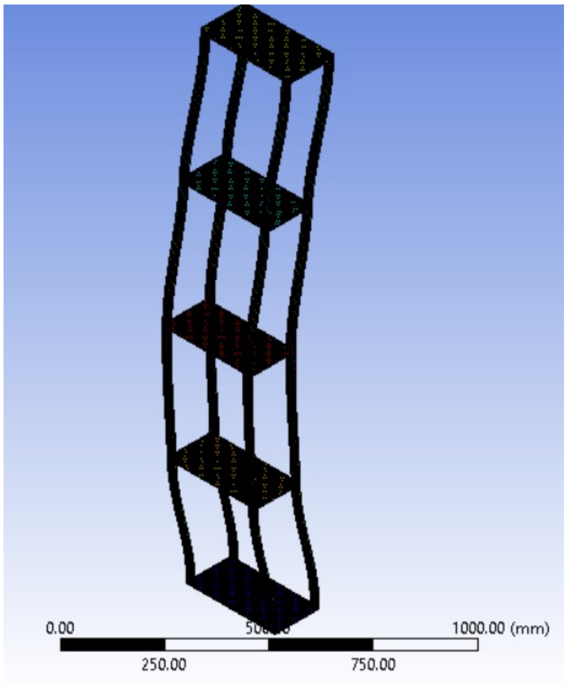

(d) Mode 4 - 15.442 Hz

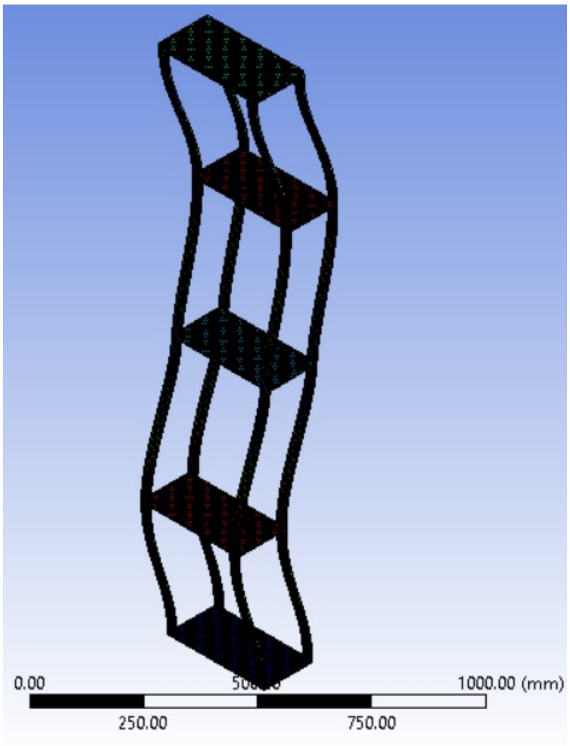

(e) Mode 5 - 27.272 Hz

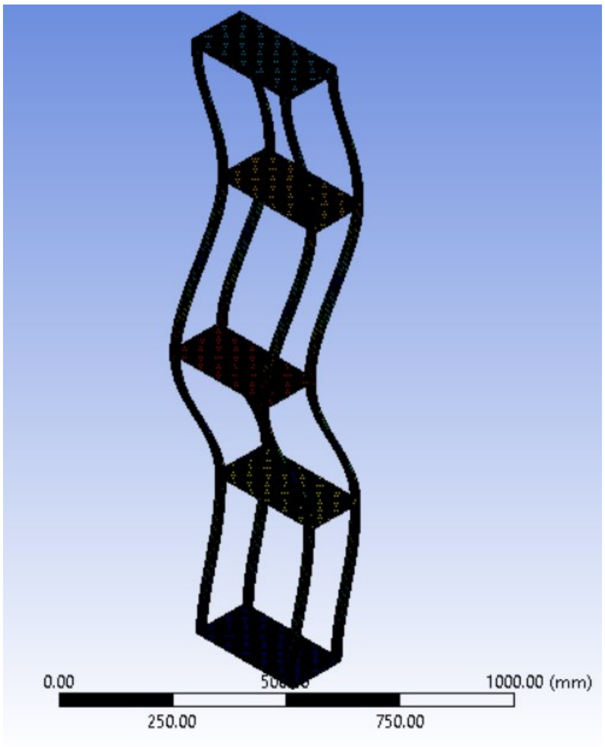

(f) Mode 6 - 37.323 Hz

Figure 26: Mode shapes and natural frequency when only 4th floor is loaded with UDL.

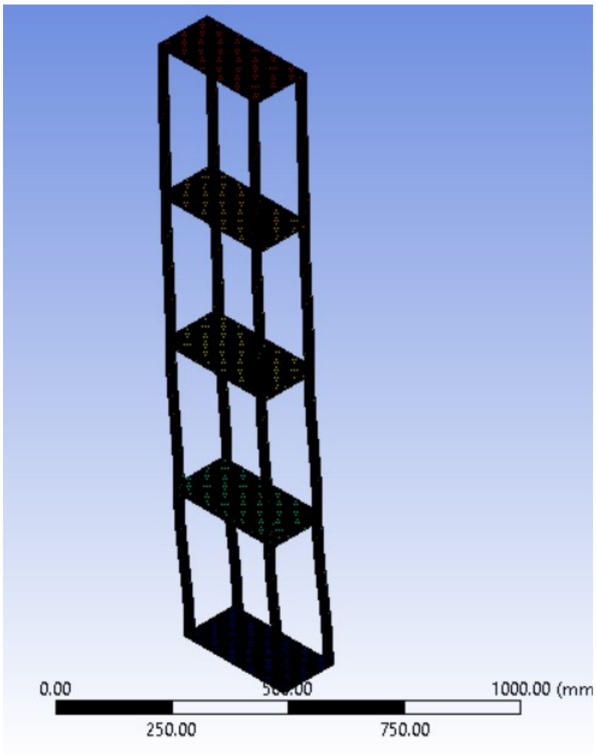

(a) Mode 1 - 5.7579 Hz

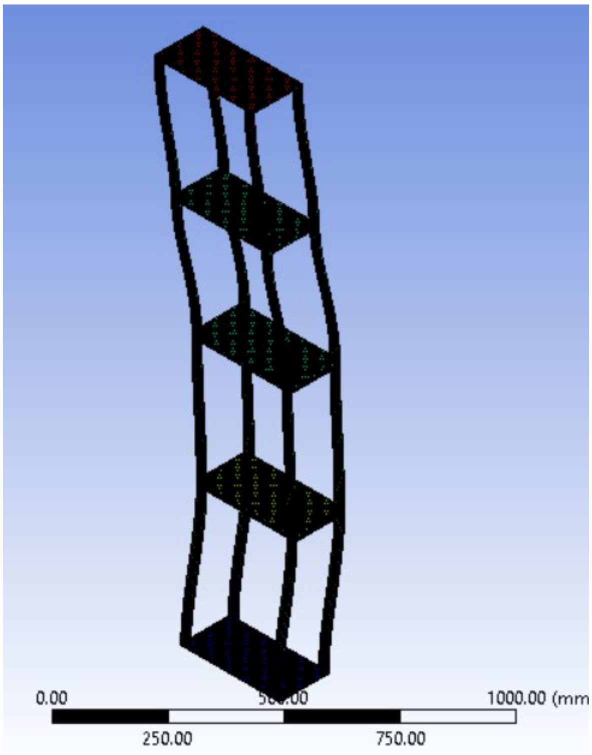

(b) Mode 2 - 14.569 Hz

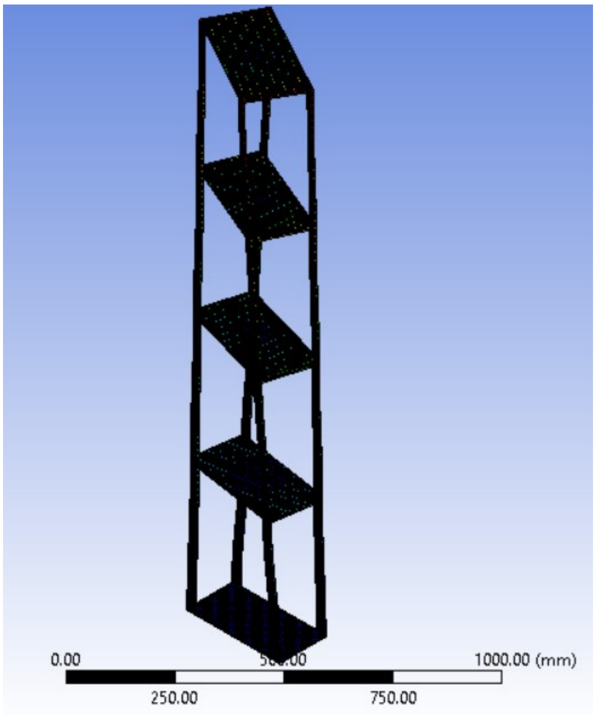

(c) Mode 3 - 16.69 Hz

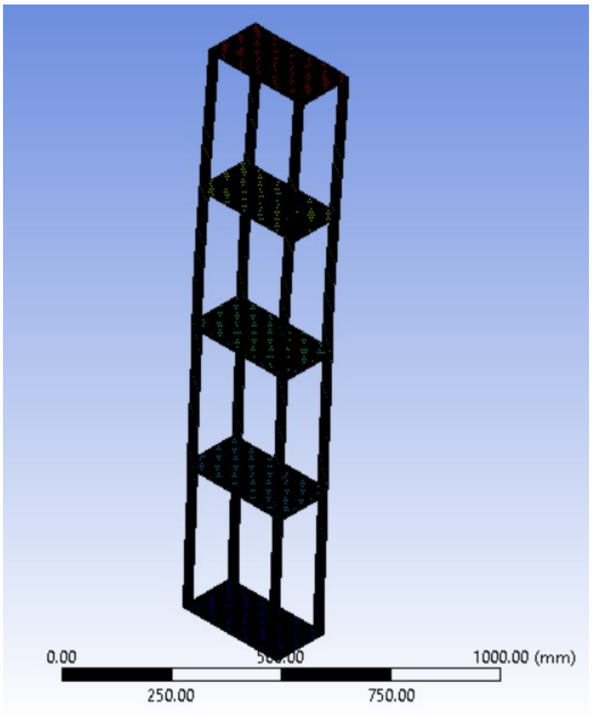

(d) Mode 4 - 19.611 Hz

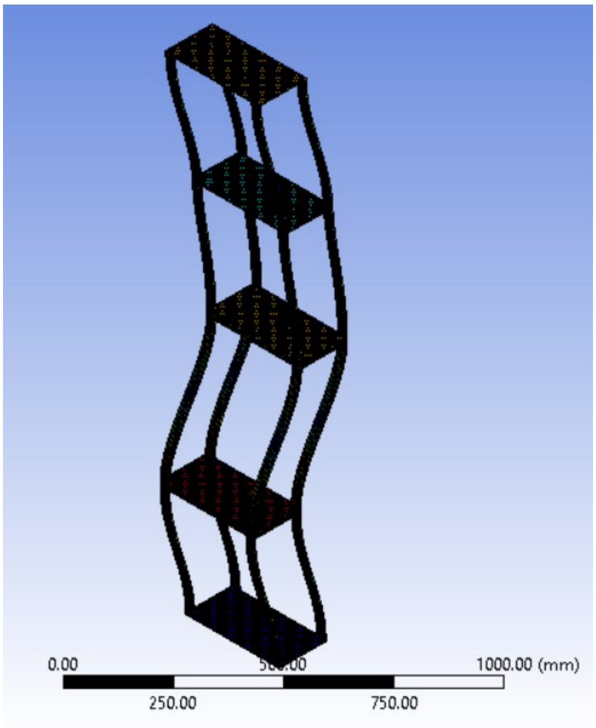

(e) Mode 5 - 22.529 Hz

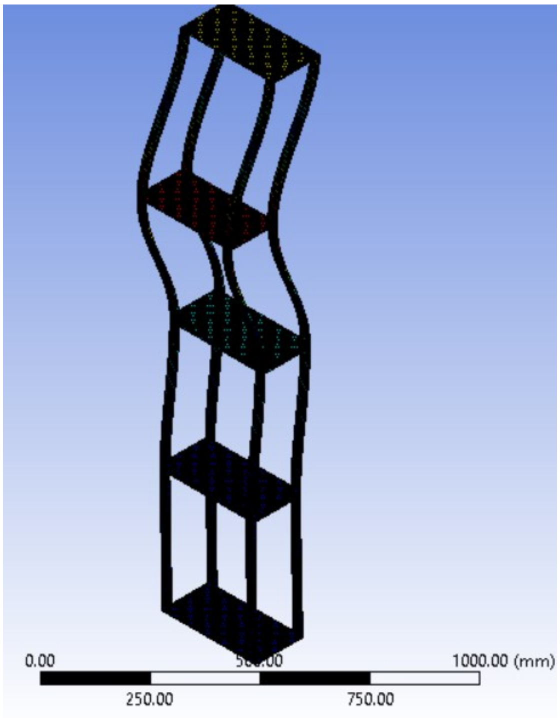

(f) Mode 6 - 34.208 Hz

Figure 27: Mode shapes and natural frequency when only 1st and 2nd floors are loaded with UDL.

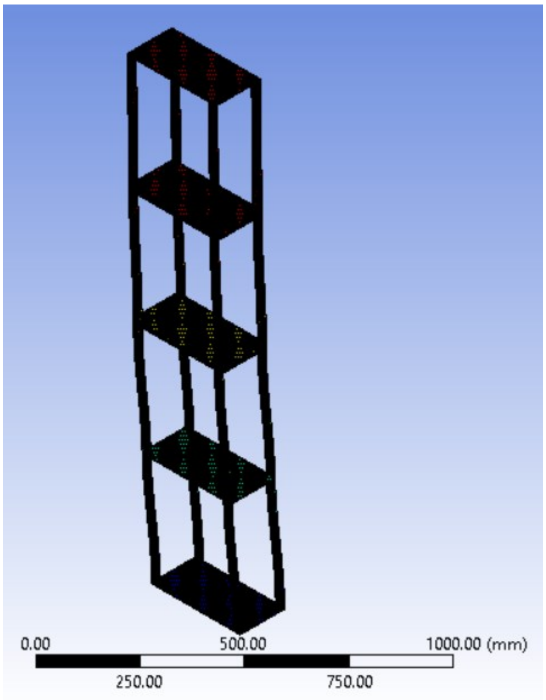

(a) Mode 1 - 4.8262 Hz

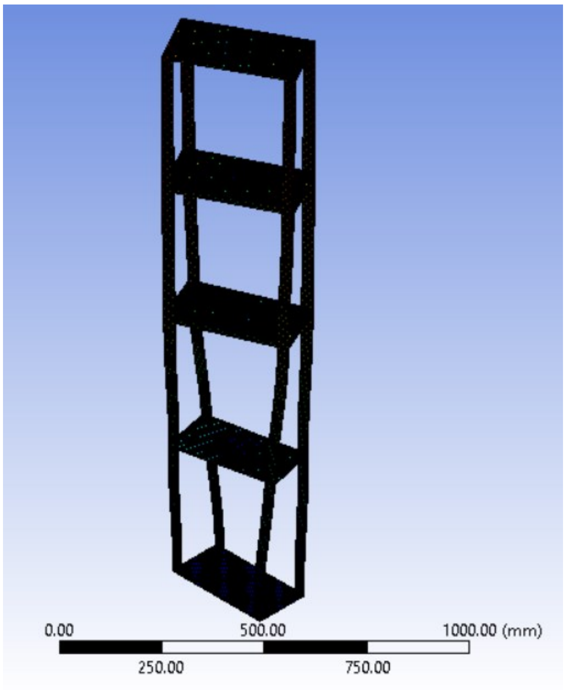

(b) Mode 2 - 12.691 Hz

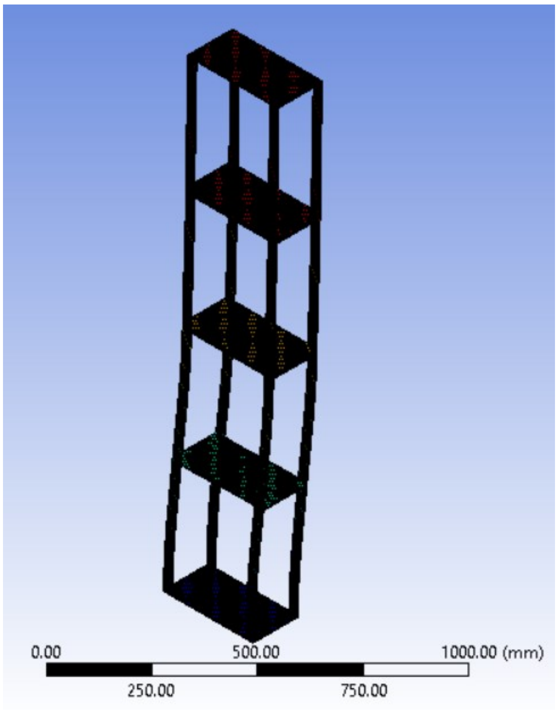

(c) Mode 3 - 14.076 Hz

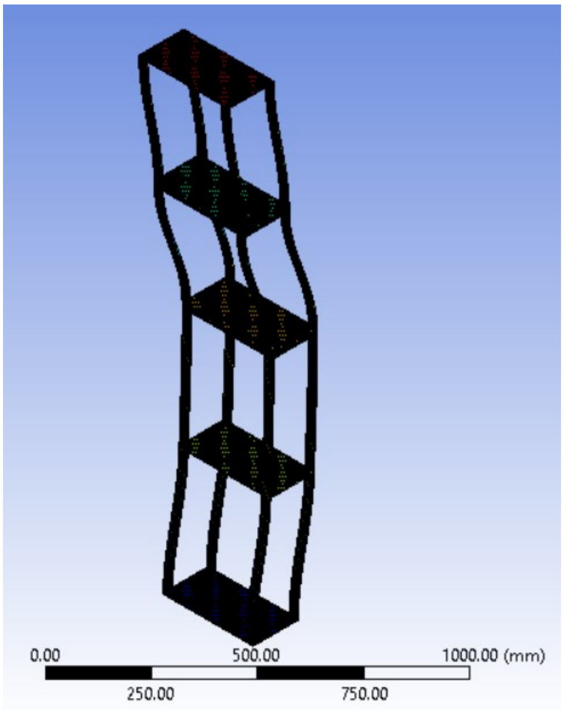

(d) Mode 4 - 16.466 Hz

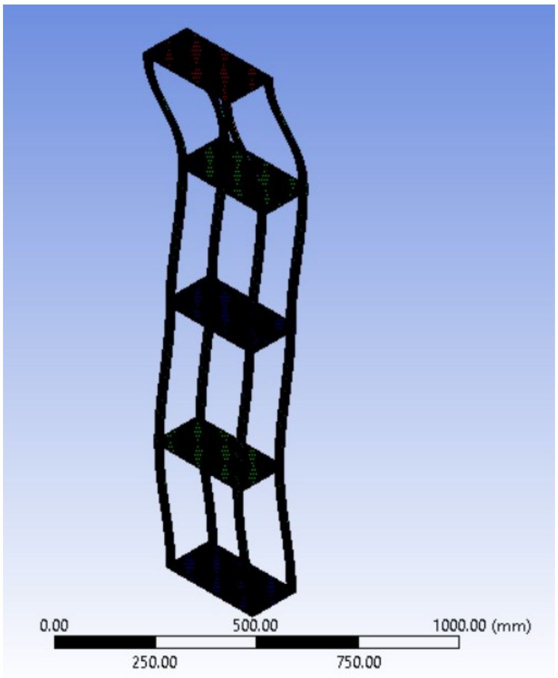

(e) Mode 5 - 26.84 Hz

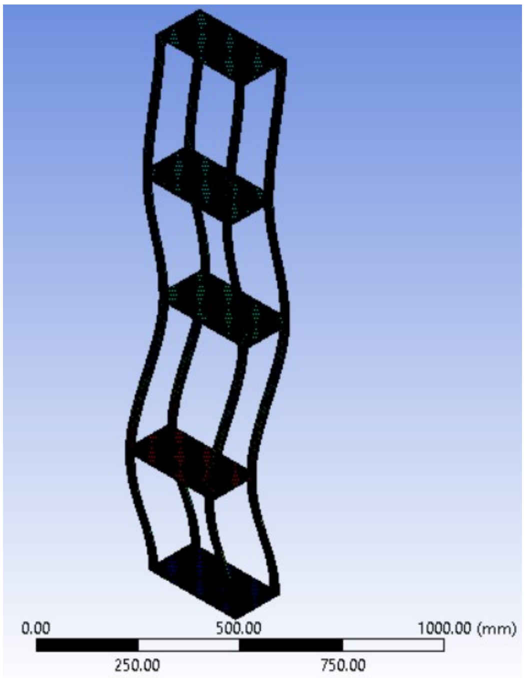

(f) Mode 6 - 30.309 Hz

Figure 28: Mode shapes and natural frequency when only 2nd and 3rd floors are loaded with UDL.

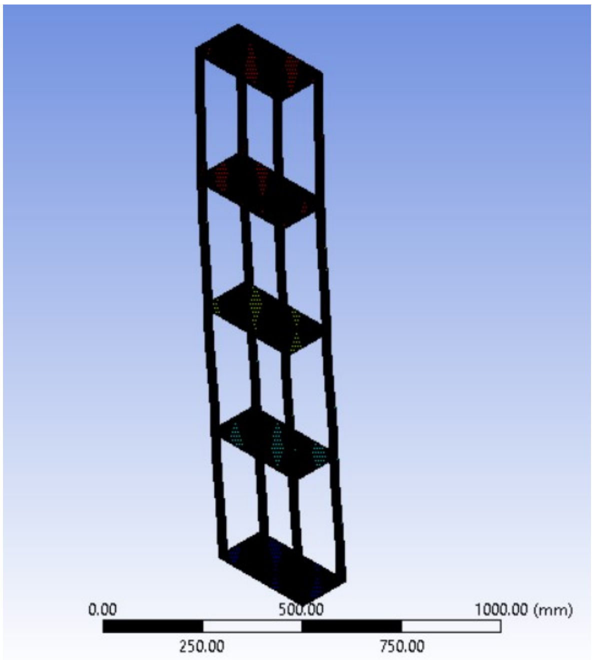

(a) Mode 1 - 4.2883 Hz

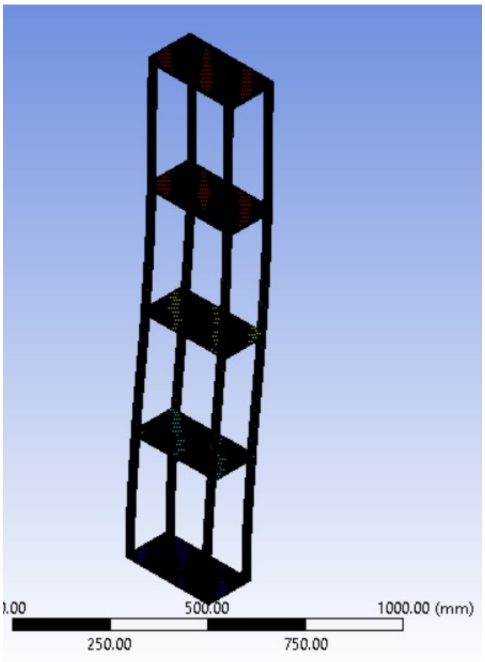

(b) Mode 2 - 9.9766 Hz

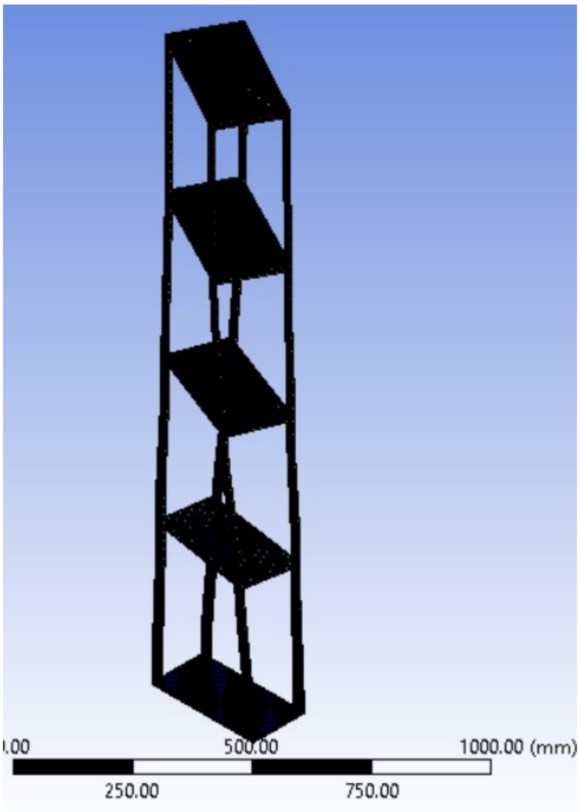

(c) Mode 3 - 10.537 Hz

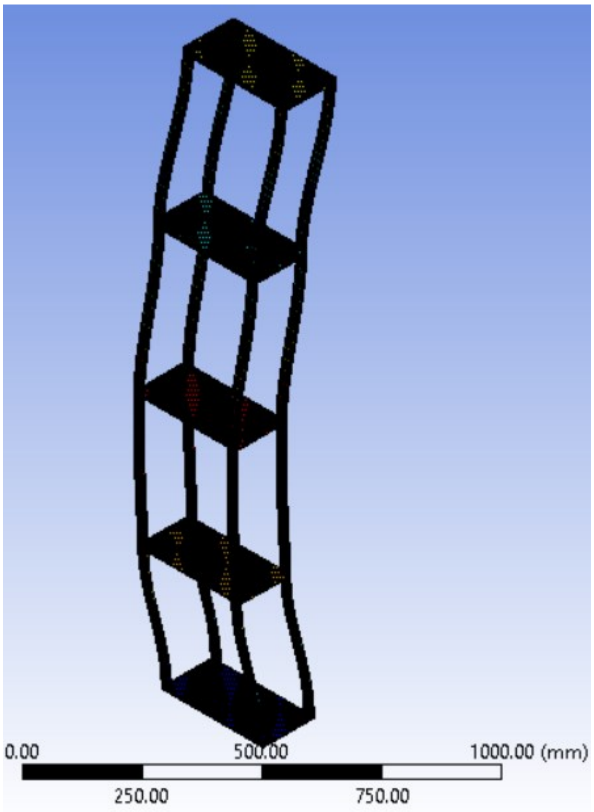

(d) Mode 4 - 16.23 Hz

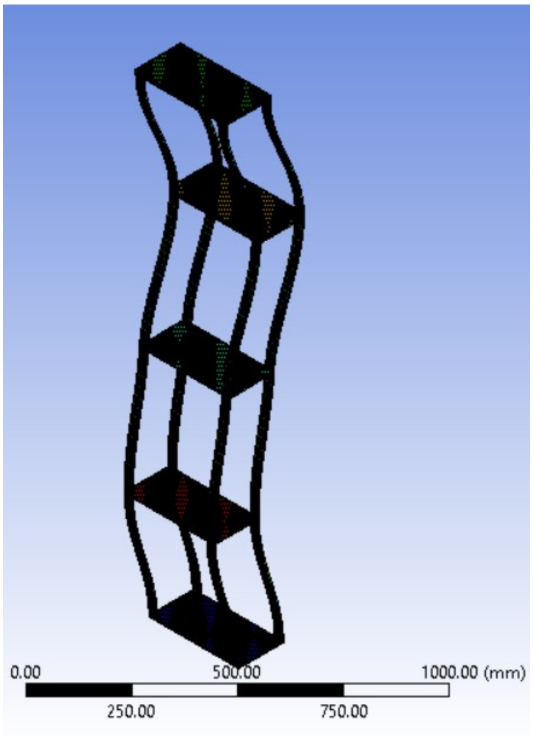

(e)Mode 5 - 22.934 Hz

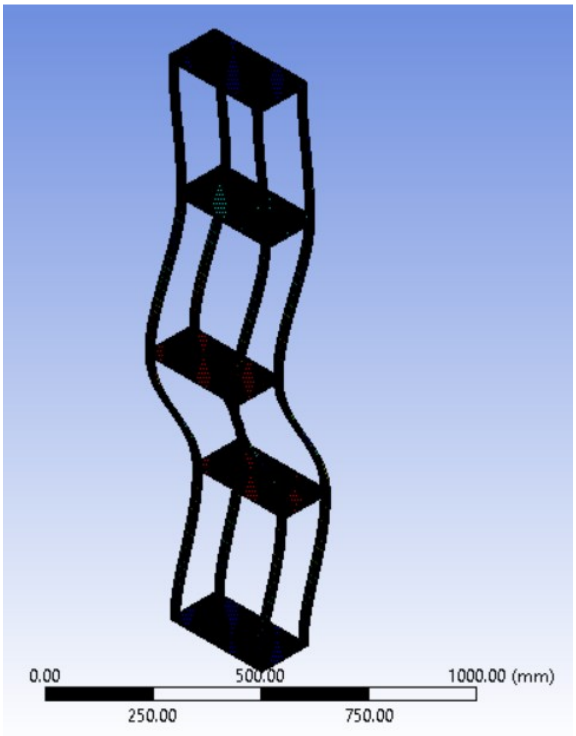

(f) Mode 6 - 35.004 Hz

Figure 29: Mode shapes and natural frequency when only 3rd and 4th floors are loaded with UDL.

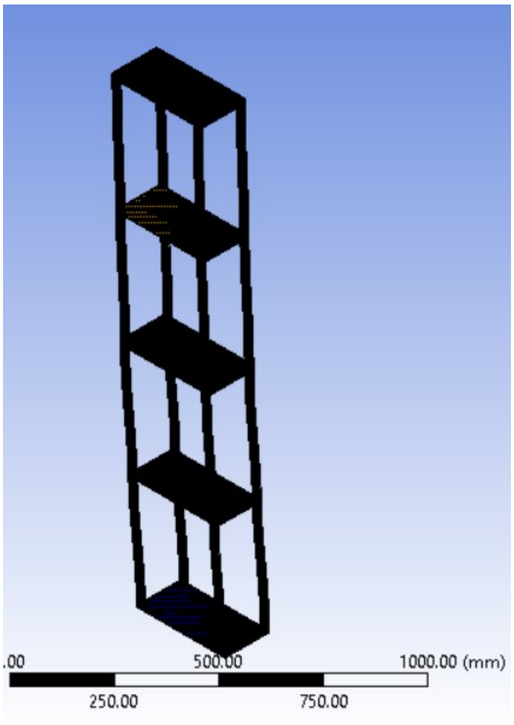

(a) Mode 1 - 4.6217 Hz

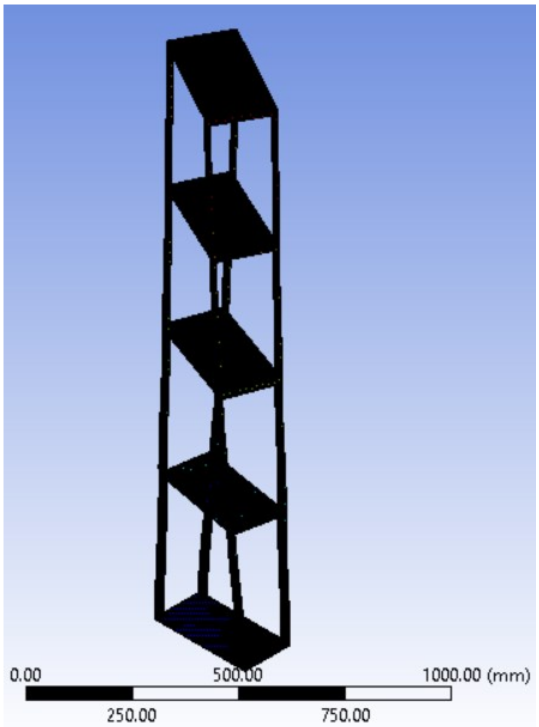

(b) Mode 2 - 11.991 Hz

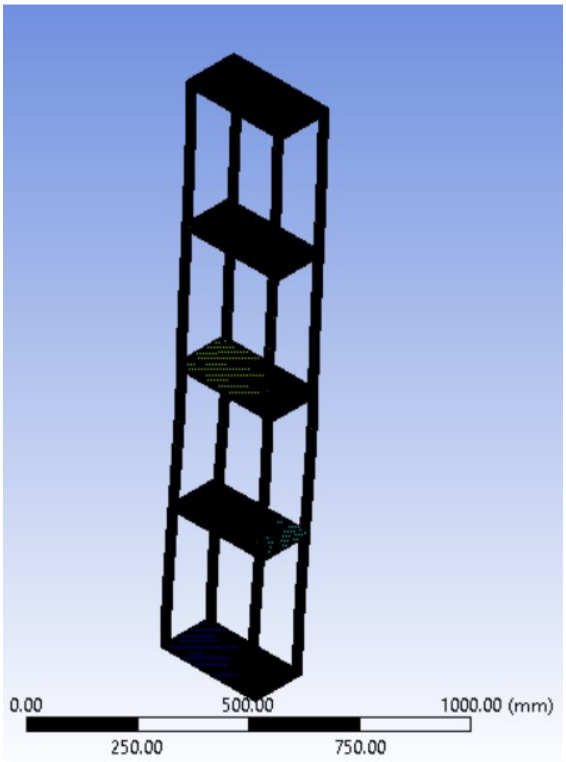

(c) Mode 3 - 12.852 Hz

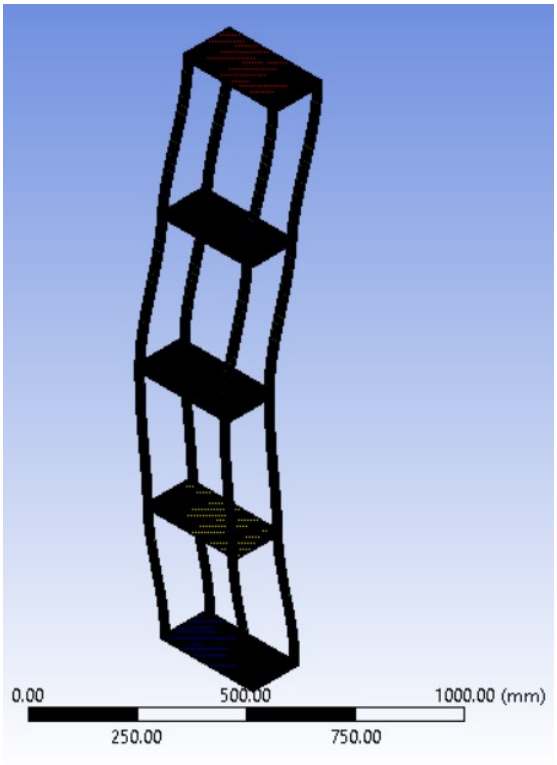

(d) Mode 4 - 13.083 Hz

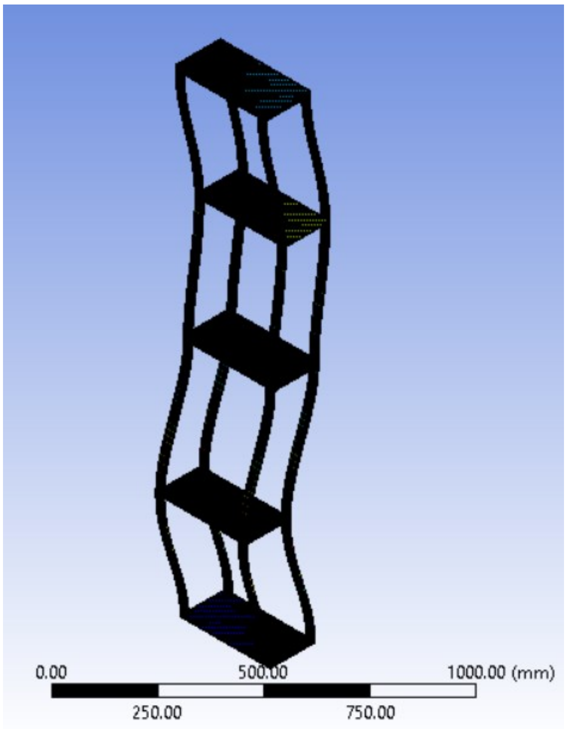

(e) Mode 5 - 28.175 Hz

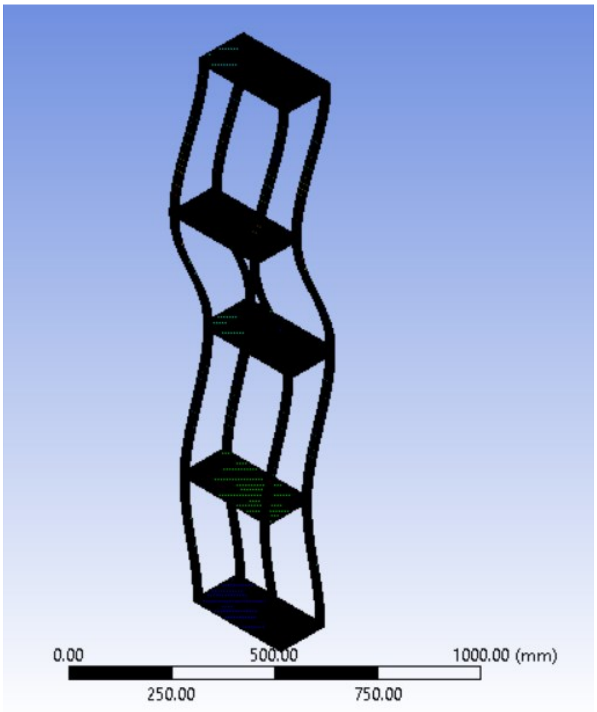

(f) Mode 6 - 32.879 Hz

Figure 30: Mode shapes and natural frequency when only 2nd and 4th floors are loaded with UDL.

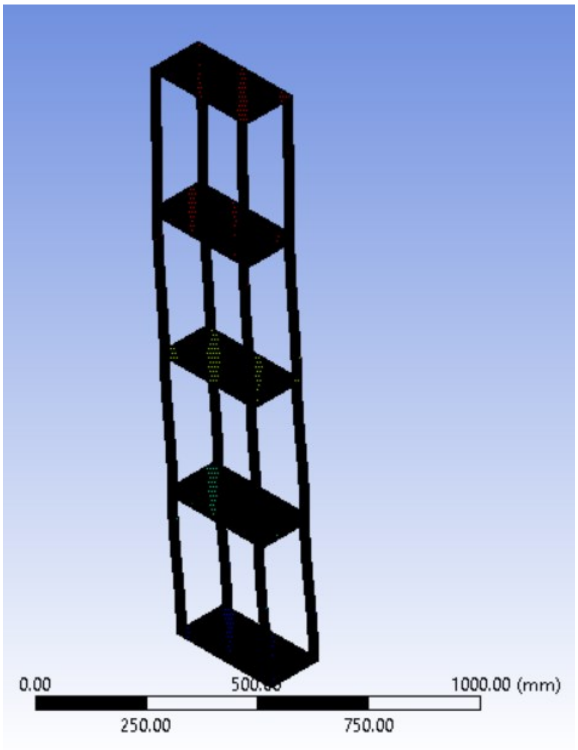

(a) Mode 1 - 5.2418 Hz

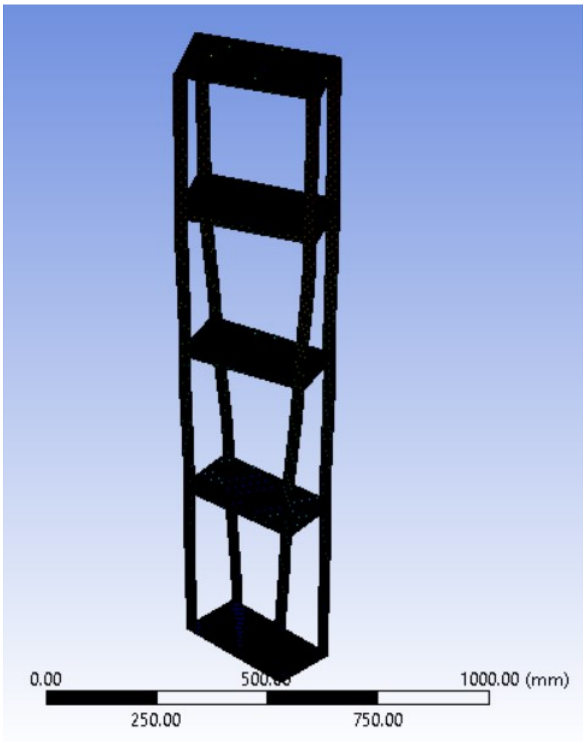

(b) Mode 2 - 14.255 Hz

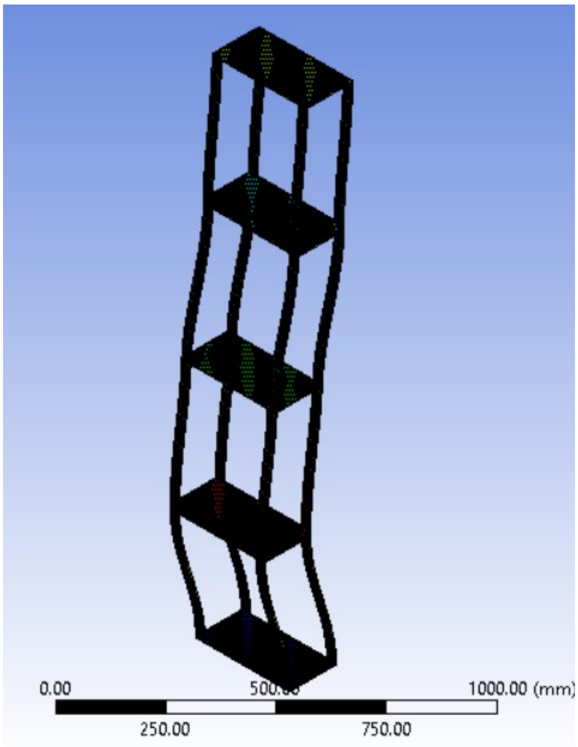

(c) Mode 3 - 15.007 Hz

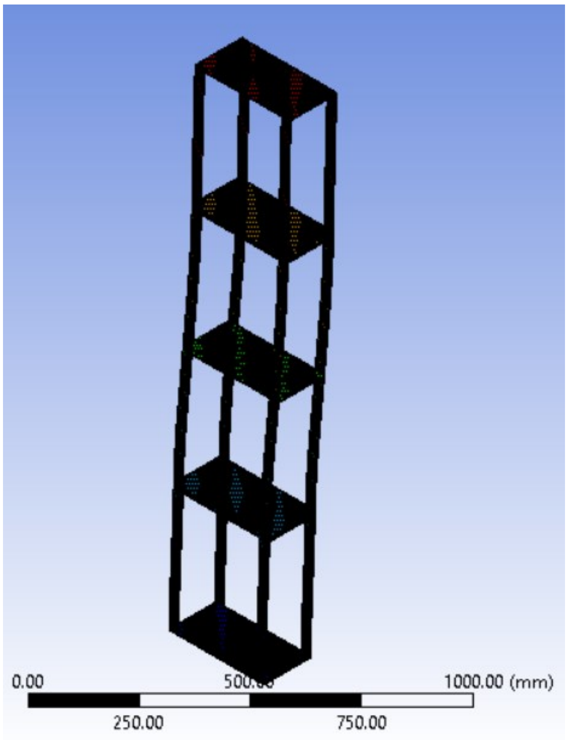

(d) Mode 4 - 16.068 Hz

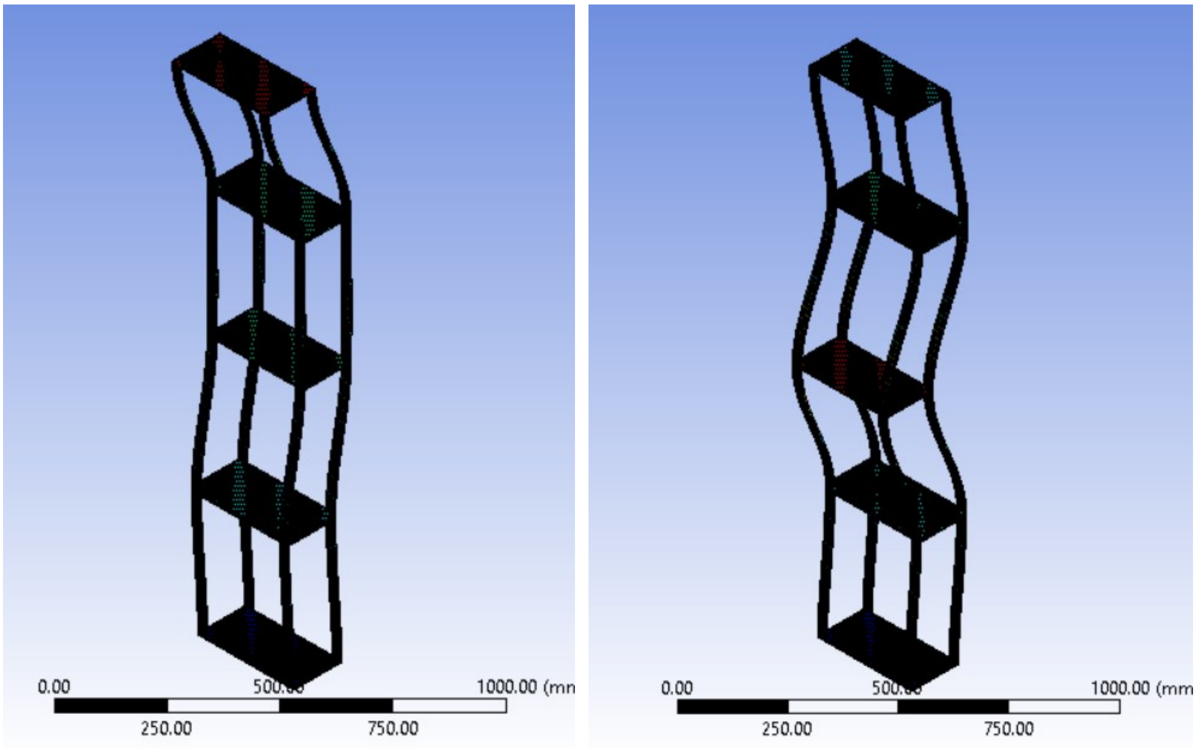

(e) Mode 5 - 25.175 Hz

(f) Mode 6 - 32.683 Hz

Figure 31: Mode shapes and natural frequency when only 1st and 3rd floors are loaded with UDL.

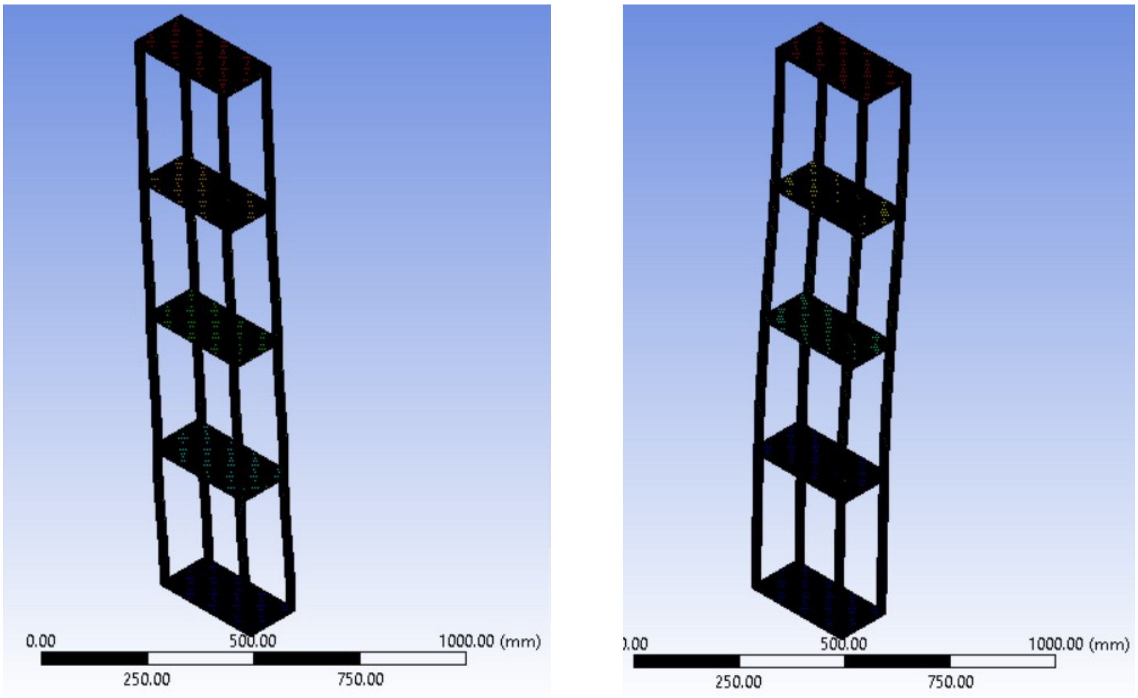

(a) Mode 1 - 4.93 Hz

(b) Mode 2 - 12.53 Hz

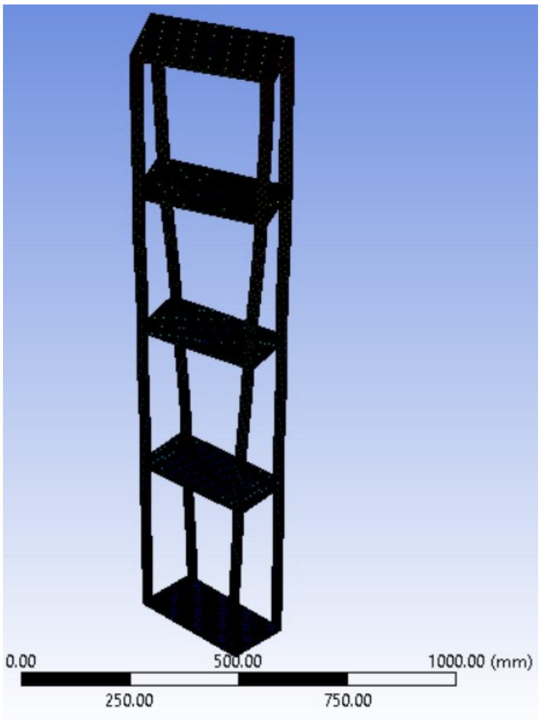

(c) Mode 3 - 12.786 Hz

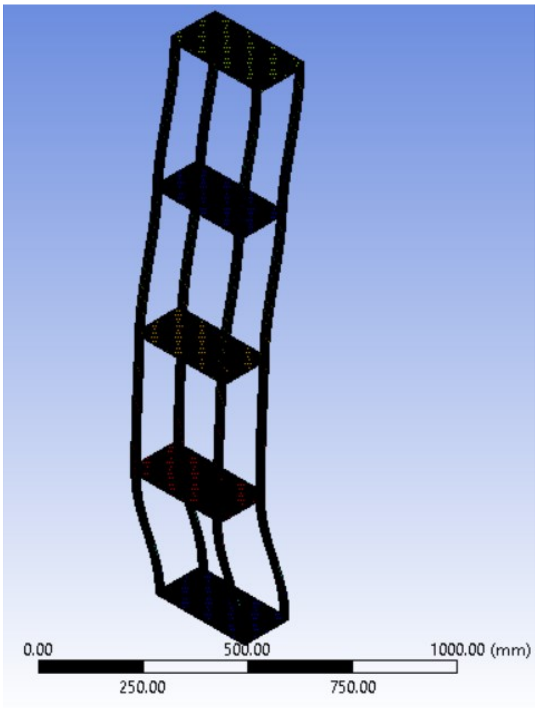

(d) Mode 4 - 13.407 Hz

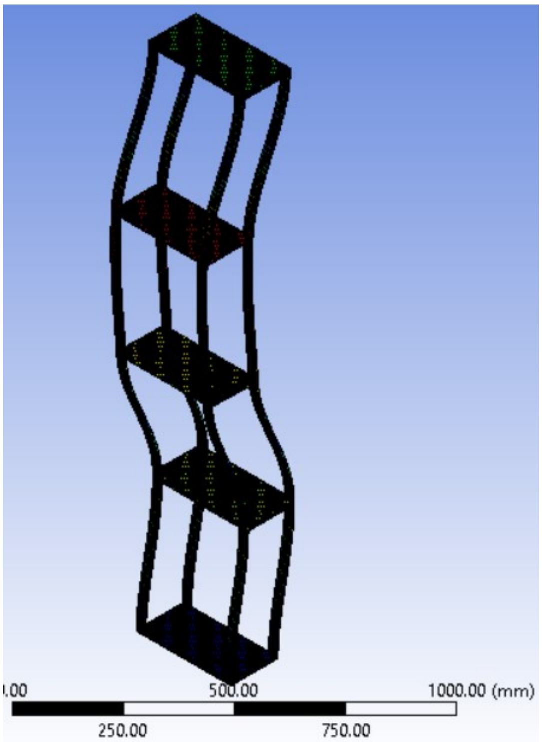

(e) Mode 5 - 23.498 Hz

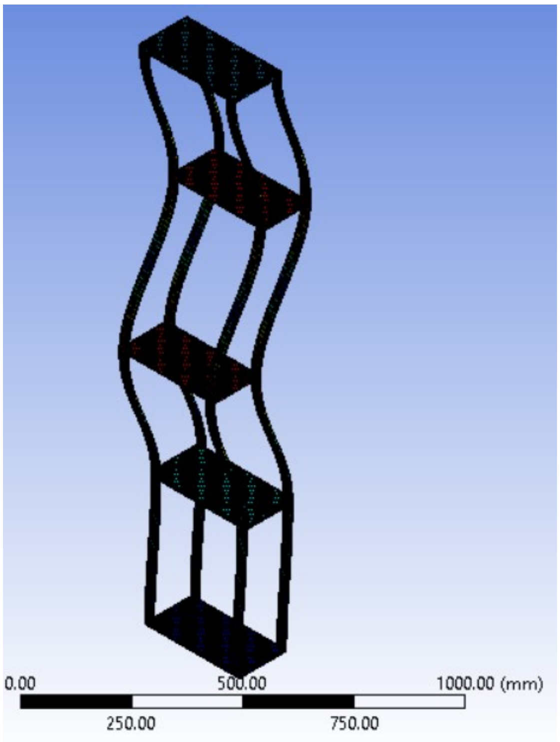

(f) Mode 6 - 36.043 Hz

Figure 32: Mode shapes and natural frequency when only 1st and 4th floors are loaded with UDL.

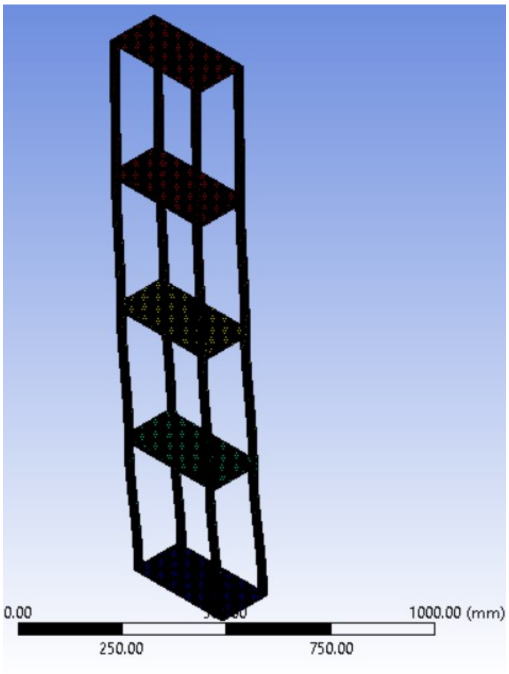

(a) Mode 1 - 5.1084 Hz

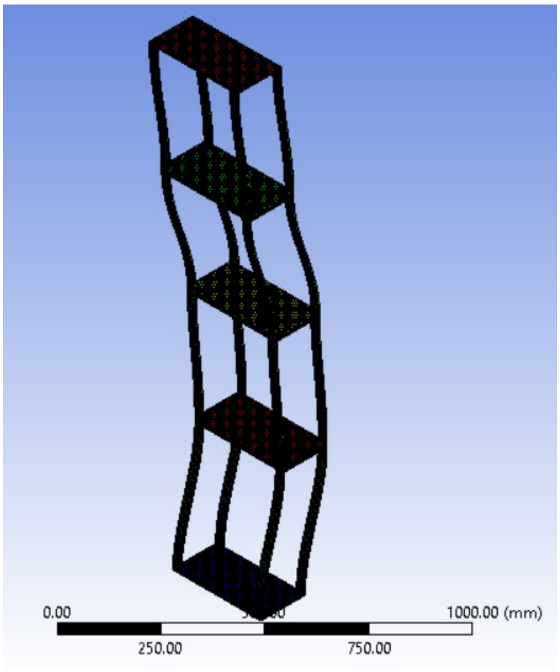

(b) Mode 2 - 14.851 Hz

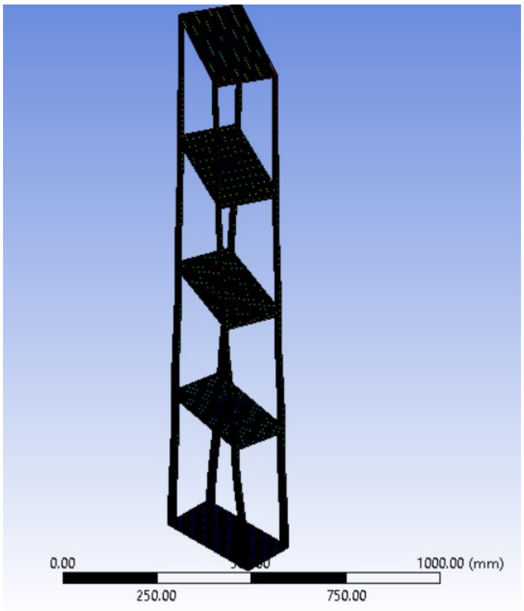

(c) Mode 3 - 16.091 Hz

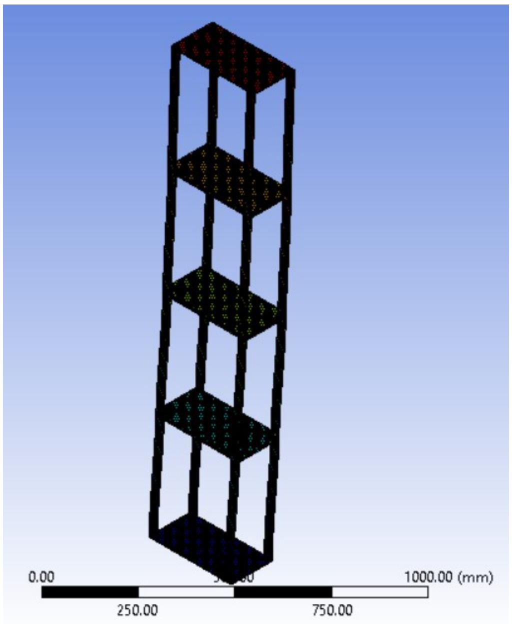

(d) Mode 4 - 19.893 Hz

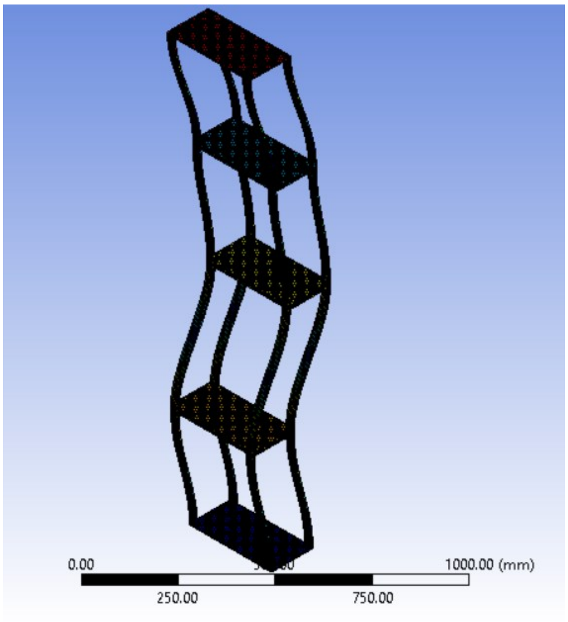

(e) Mode 5 - 23.015 Hz

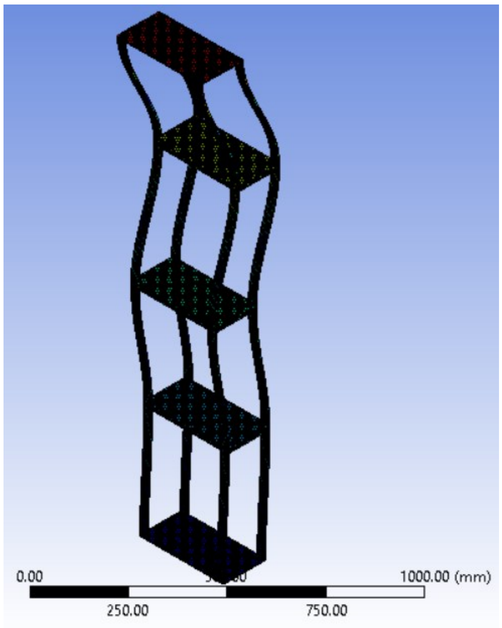

(f) Mode 6 - 27.953 Hz

Figure 33: Mode shapes and natural frequency when only 1st, 2nd and 3rd floors are loaded with UDL.

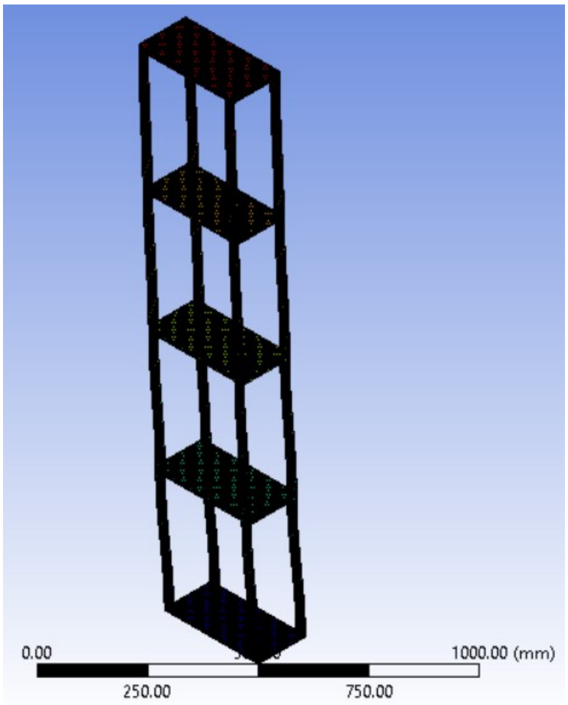

(a) Mode 1 - 4.8719 Hz

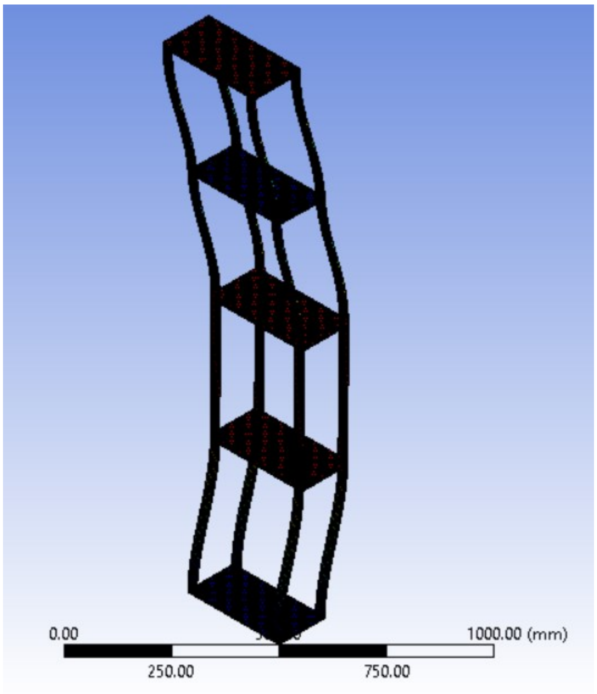

(b) Mode 2 - 12.356 Hz

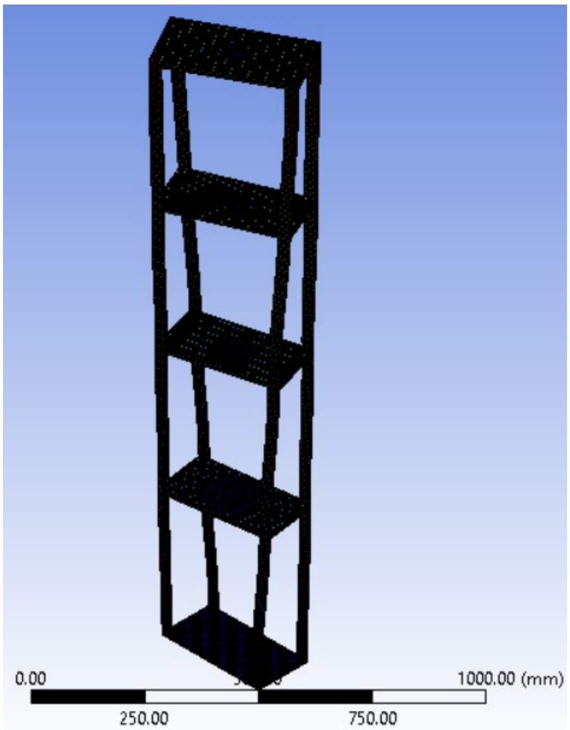

(c) Mode 3 - 14.65 Hz

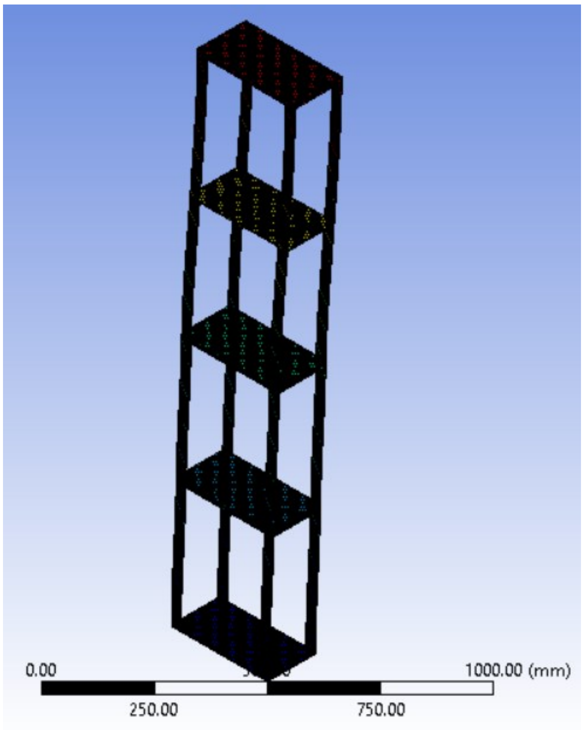

(d) Mode 4 - 16.634 Hz

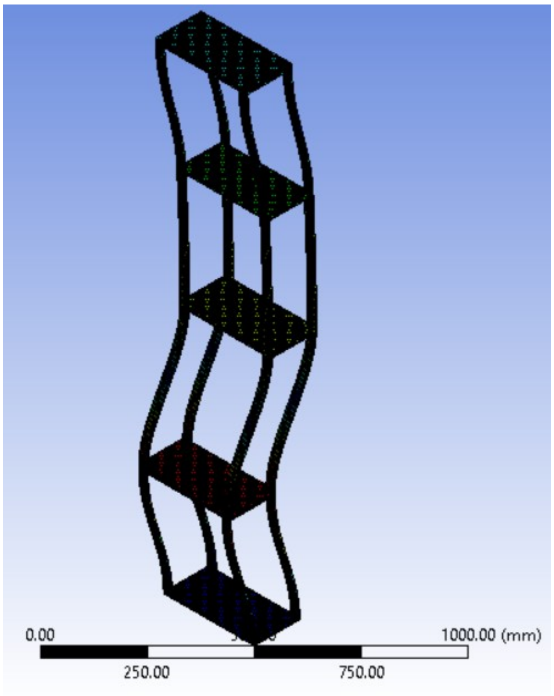

(e) Mode 5 - 21.773 Hz

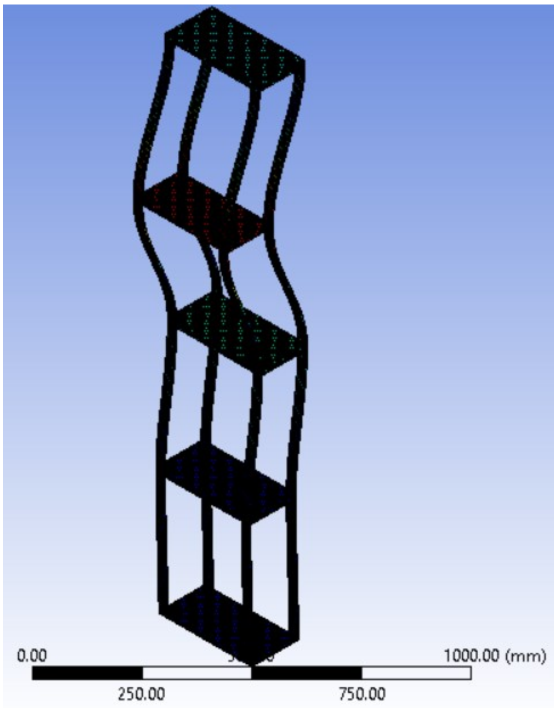

(f) Mode 6 - 32.267 Hz

Figure 34: Mode shapes and natural frequency when only 1st, 2nd and 4th floors are loaded with UDL.

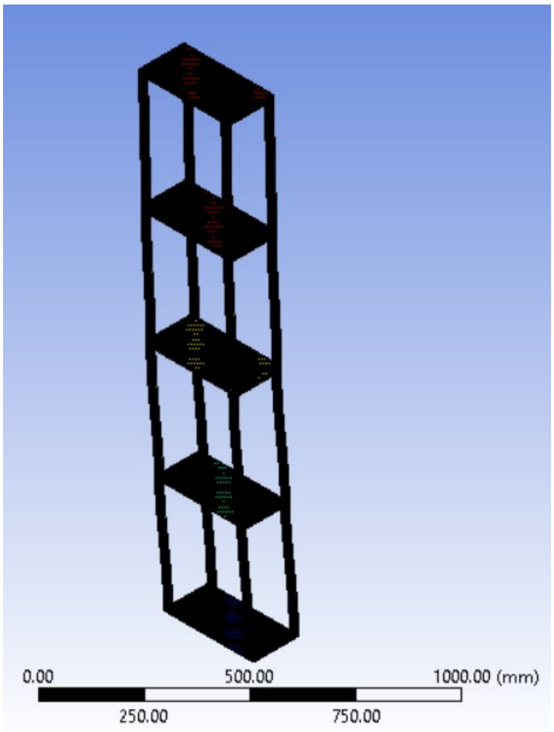

(a) Mode 1

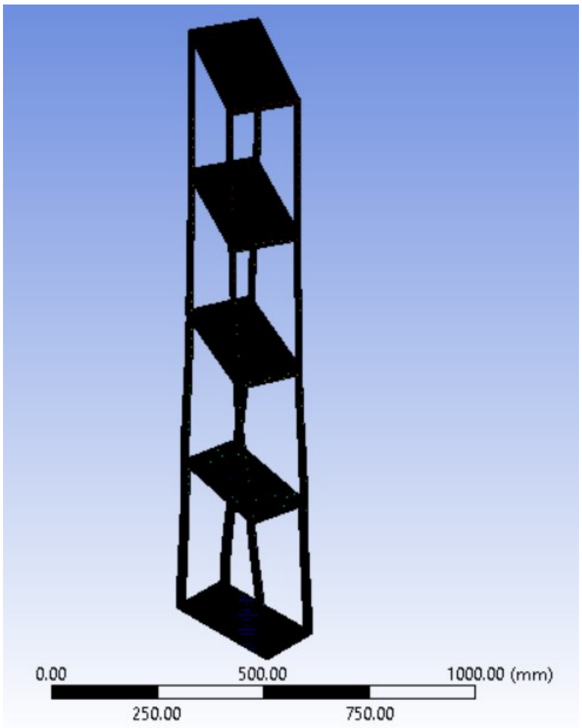

(b) Mode 2

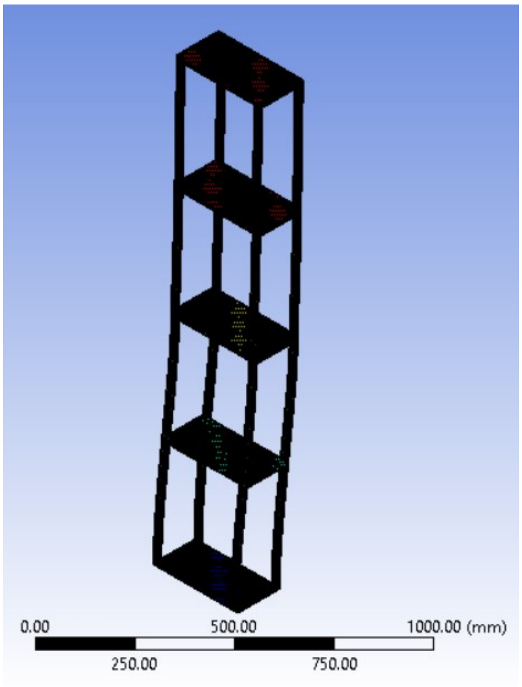

(c) Mode 3

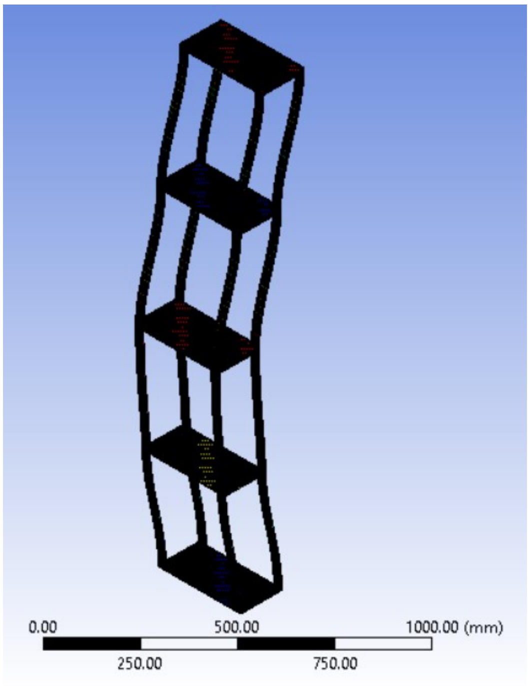

(d) Mode 4

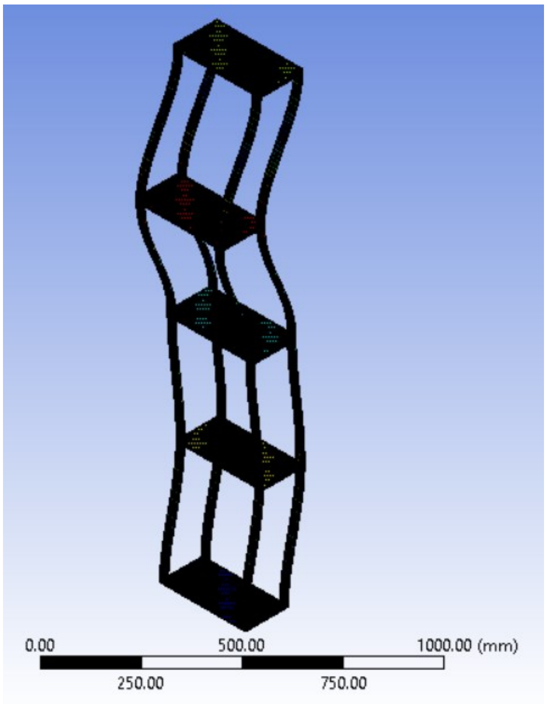

(e) Mode 5

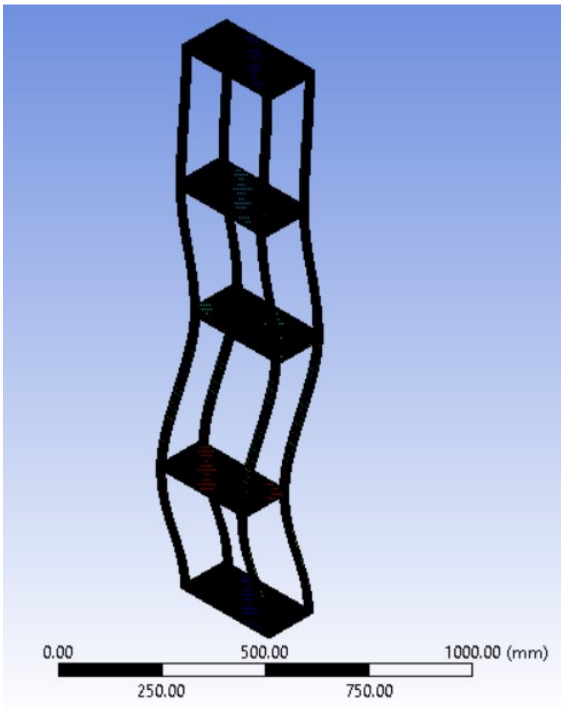

(f) Mode 6

Figure 35: Mode shapes and natural frequency when only 2nd, 3rd and 4th floors are loaded with UDL.

A.2 3D Modelling Method

All the 3D geometries have been modelled in Solidworks 2017. It is a CAD software which allows the user to generate the 3D models of the actual model in the computer environment. These models can be accurately modelled in terms of dimensions, tolerance etc.

For the research work, the model has been constructed using floors and columns. First, the bottom floor has been made and then columns have been made on top of them. The floors and columns have not been merged. Therefore, at the end, 16 bodies have been generated. This allows the simulation software to consider the floors and columns as separate entities.

A.3 Instruments

(a) Function generator [28]

(b) Oscilloscope [29]

(c) Electrodynamic Vibration Shaker and power amplifier. [30][31]

(d) Eddy current displacement sensor[32]

Figure 36: Instruments used for the experiment.

A.4 Fixing Methods

The 2-story structure has been fixed to the concrete base using 12 wall bolts. At first, the holes have made in the base plate of the structure then drilling has been done on the concrete base. Then the structure has been rigidly bolted down. The wall bolts have been made from ordinary grade steel. The wall bolts are self-tightening. So, when the nut is locked, the metal jacket expands into the concrete and grabs on to it to form a very tight joint. Each bolt can bear up to 0.3 kN in tension and 0.3 kN in shear.

(a) Assembled wall bolt

(b) Diamantled wall bolt

Figure 37: Wall bolts used in fixing the structure to the concrete base.

CD